Title: Lectin-Seq: a method to profile lectin-microbe interactions in native communities

Authors: Robert L. McPherson[1,2]†, Christine R. Isabella[1,2]†, Rebecca L. Walker[3], Dallis Sergio[3], Sunhee Bae[1], Tony Gaca[3], Smrithi Raman[1], Le Thanh Tu Nguyen[2,6], Darryl A. Wesener[4,5], Melanie Halim[1,2], Michael G. Wuo[1,2], Amanda Dugan[1,2], Robert Kerby[7], Soumi Ghosh[8], Federico E. Rey[7], Catherine Dhennezel[3], Gleb Pishchany[3], Hera Vlamakis[2,3], Eric J. Alm[2,3,6], Ramnik J. Xavier[2,3,9], and Laura L. Kiessling[1,2]*

Affiliations:

[1] Department of Chemistry, Massachusetts Institute of Technology; Cambridge, MA 02139, USA.

[2] Center for Microbiome Informatics and Therapeutics, Massachusetts Institute of Technology, Cambridge; MA 02139, USA.

[3] The Broad Institute of MIT and Harvard; Cambridge, MA 02142, USA.

[4] Edison Family Center for Genome Sciences and Systems Biology, Washington University School of Medicine; Saint Louis, MO 63110, USA.

[5] Center for Gut Microbiome and Nutrition Research, Washington University School of Medicine; Saint Louis, MO 63110, USA.

[6] Department of Biological Engineering, Massachusetts Institute of Technology; Cambridge, MA 02139, USA.

[7] Department of Bacteriology, University of Wisconsin-Madison; Madison, WI 53706, USA.

[8] Department of Biology, Massachusetts Institute of Technology; Cambridge, MA 02139, USA.

[9] Center for Computational and Integrative Biology, Department of Molecular Biology, Massachusetts General Hospital, Harvard Medical School; Boston, MA 02114, USA.

*Correspondence to: kiesslin@mit.edu

† These authors contributed equally to this work

Abstract: Soluble human lectins are critical components of innate immunity. Genetic models suggest lectins influence host-resident microbiota, but their specificity for commensal and mutualist species is understudied. Elucidating lectins' roles in regulating microbiota requires an understanding of which microbial species they bind within native communities. To profile human lectin recognition, we developed Lectin-Seq. We apply Lectin-Seq to human fecal microbiota using the soluble mannose-binding lectin (MBL) and intelectin-1 (hItln1). The microbial interactomes of MBL and hItln1 differ in composition and diversity. MBL binding is highly selective for a small subset of species commonly associated with humans. In contrast, hItln1's interaction profile encompasses a broad range of lower-abundance species. Our data uncover stark differences in the commensal recognition properties of human lectins.

One-Sentence Summary: Soluble human lectins bind distinct bacterial species in fecal microbiota.

Main text:

Introduction

Humans host trillions of microbes (*1*), but the mechanisms we use to recognize and distinguish between different microbial species are not fully defined. Microbes are decorated with cell surface glycans that act as a primary point of contact between host and microbe (*2*). Microbial glycan composition is unique between species and could serve as a molecular readout of cellular identity for host factors (*3*). Soluble human carbohydrate-binding proteins termed lectins distinguish cell surface glycans and can achieve species- and strain-level binding specificity (*4-6*). Lectins are implicated in immune defense against pathogens, and lectin-microbe interactions can be key determinants of cell fate for microbial pathogens (*7, 8*). Genetic models suggest lectins play notable roles in regulating broad groups of microbial species in the gut microbiota (*9-12*). However, the microbial specificity of human lectins in host-resident communities has not been elucidated. Critically, it is unclear whether lectins in such communities bind a wide range of species or restrict their interactions to select microbes. Such information is vital to developing a mechanistic understanding of how lectins regulate the microbiota.

Lectins are commonly classified by their monosaccharide specificity, but their cell binding specificity can be influenced by glycan accessibility, density and secondary interactions (*13*). In some cases, monosaccharide specificity can be used to predict lectin-microbe interactions (*14*), but we postulate that other features of cell surface glycan display influence recognition. Previous studies have primarily characterized lectin-microbe interactions using monoculture binding assays (*11, 14*). Single-species binding assays have drawbacks: bacteria can modulate their glycan displays under different growth conditions potentially leading to differences in the glycan composition of native and cultured microbes (*15, 16*). Moreover,

relevant lectin binding occurs in mixed communities. We postulate that competition for lectin binding might occur in such physiologically relevant settings.

Results

To assess lectin selectivity within mixed communities, we first evaluated the binding of the human lectin intelectin-1 (hItln1) to bacterial isolates from the human gut microbiota. Previously, we found hItln1 exhibits serotype-specific binding to isolates of *Streptococcus pneumoniae* (*14*). Others have noted binding to different bacterial species considered pathogenic, suggesting hItln1 targets pathogens (*17, 18*). Since hItln1 is expressed in the small intestine (*19*), we assessed the binding of recombinant hItln1 to a collection of human gut microbial strains by flow cytometry. The lectin binds to strains from diverse phyla (Fig. 1A-B; Table S1). The ability of hItln1 to bind to gut-resident species that can contribute to human health emphasizes the need to further characterize human lectin binding to commensal and mutualist microbes.

The ability of a lectin to bind an individual microbial species may not be representative of its specificity in physiological settings, especially for those lectins like hItln1 that are localized at mucosal barriers. We therefore generated a synthetic community from two binding species (*Escherichia fergusonii* and *Lactobacillus reuteri*) and two non-binding species (*Bacteroides ovatus* and *Proteus penneri*) that were each distinguishable by their scattering properties (Fig. 1A-B). In this mixed community of 50% hItln1 binders (Fig. 1C), the lectin bound to only 29.6% of cells. Even at higher hItln1 concentrations, 50% binding was never achieved (Fig. S1A). The forward scatter (FSC) and autofluorescence (FL1-H; FITC) profile of the hItln1-bound population matches that of *L. reuteri* (Fig. 1A-C, Fig. S1B-D), indicating that *L. reuteri* outcompetes *E. fergusonii* for htln1 binding in this simple mixed community. These data show that lectin selectivity can be altered by the species composition of microbial mixtures. Notably, the composition of human-resident microbial communities varies between individuals;

thus, understanding human lectin function requires assessing recognition within diverse communities. These findings provide impetus to profile lectin binding to bacterial species within native communities.

We next characterized the binding specificity of two lectins in native microbial communities. The human gut harbors the most complex and diverse microbial community associated with the human body, and snapshots of the community are readily accessible through stool (*20*). We queried binding by hItln1, as its expression in the gut (*19*), its biochemical affinity for glycans exclusively found on microbes (*14, 21*), and our initial binding data (Fig. 1) all suggest it may preferentially interact with gut-resident microbes. Additionally, hItln1 is associated with diseases linked to microbiome dysbiosis, suggesting it may regulate gut microbiota (*22, 23*). However, interactions between hItln1 and intestinal microbial communities have not been assessed.

To contrast with our studies of hItln1, we also evaluated the specificity of human mannose-binding lectin (MBL) for human gut microbial communities. Decades of research show that MBL binding promotes pathogen clearance (*24-26*) supporting a role in immune defense. A deficiency of MBL in murine models causes changes in the gut microbiota (*12*), but whether these changes are due to direct MBL-microbe interactions is unclear. MBL is primarily expressed in the liver, but low levels of expression have been detected in the intestine (*27*). An understanding of the direct interactions between MBL and gut-resident microbes is needed to interpret its influence on microbiome regulation.

We used flow cytometry to analyze the binding of recombinant MBL and hItln1 to stool homogenates collected from healthy human donors (Fig. 2A). Both lectins were tested with calcium because they require calcium for glycan binding (*28, 29*). We assessed MBL and hItln1 at a range of concentrations (Fig. S2A-B) and found each bound a substantial population of intact

microbial cells (Fig. 2B, middle column; Fig. 2C). MBL binding was saturated at ~20 μg/mL where it bound 10-20% of cells in stool homogenate (Fig. 2B, middle column; Fig. 2C; Fig. S2B). HItln1 interacted with a comparable proportion of cells at 10 and 20 μg/mL (Fig. 2B, middle column; Fig. 2C; Fig. S2B-C) therefore, all subsequent experiments used this lectin concentration. The addition of the calcium chelator ethylenediaminetetraacetic acid (EDTA) reduced binding (Fig. 2B, right column). Lectin-specific inhibitors - mannan for MBL (*5*) or glycerol for hItln1 (*14*) – also were inhibitory (Fig. S3A-B). These findings indicate that the detected microbial binding interactions are glycan dependent. The addition of recombinant human lectins is a critical aspect of this analysis. We did not detect notable levels of endogenous MBL and hItln1 on the tested human samples (Fig. S4A-B). These oligomeric lectins bind through multivalent interactions, which are kinetically labile. Thus, the lectins should be washed away during the stool homogenization process. Indeed, application of the stool homogenization conditions to lectin-treated samples reduced binding of recombinant MBL or hItln1 (Fig. S4C).

MBL and hItln1 bind orthogonal sets of glycans on a microbial glycan array (Fig. 2D; Table S2). HItln1 enriched for glycans with 3-deoxy-D-*manno*-oct-2-ulosonic acid (KDO), D-*glycero*-D-*talo*-oct-2-ulosonic acid (KO), D-glycerol 1-phosphate, and galactofuranose residues (*14, 21*) (Table S2), epitopes that are absent from mammalian glycomes but widely distributed in bacteria (*30*). In contrast, MBL preferentially bound glycans containing mannose and N-acetyl glucosamine residues, and a recent study suggests that 10-30% of murine stool microbiota display mannose and N-acetylglucosamine (*31*). Thus, hItln1 and MBL form glycan-dependent interactions with substantial proportions of human stool microbiota. Despite their similar levels of bacterial engagement (Fig. 2C), we hypothesized the lectin's orthogonal glycan recognition properties would translate to specificity for different microbes. To test this possibility, we co-incubated fluorescently labeled MBL and hItln1 with healthy human stool homogenate and

analyzed binding by flow cytometry. Most lectin-bound cells were bound by either MBL or hItln1 with less than 5% binding both (Fig. 2E-F). Thus, MBL and hItln1 bind distinct bacterial populations.

Our next objective was to identify the microbial taxa recognized by each lectin. To maximize microbial diversity in our analyses we included stool homogenate from 5 healthy and 9 clinically diagnosed inflammatory bowel disease (IBD) patient donors. Although the composition of healthy and IBD microbiomes differ (*32*), similar levels of lectin binding occurred between healthy and diseased samples (Fig. S5A). Stool homogenates from these 14 donors were stained with MBL or hItln1, and the lectin-bound and unbound cells were isolated by fluorescence-activated cell sorting (FACS). The sorted fractions were analyzed by metagenomic sequencing and assigned species-level taxonomy using MetaPhlAn2.0 (*33*) to determine the relative abundance of microbial species in each fraction. Finally, we calculated a probability ratio (P_R) (*34*) for each species to determine if it was enriched or depleted in the lectin-bound fraction. We refer to this workflow as Lectin-Seq (Fig. 3).

The microbe-binding properties of MBL were remarkably specific. Lectin-Seq revealed that MBL-bound fractions were predominantly composed of *Faecalibacterium prausnitzii* (Fig. 4A, Fig. S6; Table S4). *F. prausnitzii* was present in the MBL-bound fractions of 12/14 stool samples and on average accounted for >40% relative abundance across all MBL-bound fractions (Fig. 4A-B; Fig. S6). In the two remaining samples, we did not detect *F. prausnitzii* in the input fraction (Fig. 4B). In stool samples that contain *F. prausnitzii*, the microbe was enriched in the MBL-bound fraction of 8/12 samples as indicated by a positive P_R (Fig. 4C). In the remaining 4 samples *F. prausnitzii* had a negative P_R close to zero indicating that this microbe was present at similar levels in the MBL-bound and unbound fraction (Fig. 4C).

F. prausnitzii is an abundant member of the gut microbiota; in the samples analyzed, the average percent relative abundance was ~12% (Table S4). To determine if MBL recognition correlates with species abundance, we asked if the MBL-bound fraction was enriched for other abundant species. Out of the top 10 most abundant species (average abundance in input fraction; Fig. S7A) only *F. prausnitzii* had an average $P_R > 0$ for the MBL-bound fraction, indicating that MBL binding does not track with species abundance (Fig. 4D). MBL enriched for an additional 35 lower relative abundance species (average input abundance <0.01); however, more than half of these species occur in only one stool sample (Table S4; Fig. S8A).

Only two species apart from *F. prausnitzii* that were enriched by MBL in least five samples – *Akkermansia muciniphila* and *Ruminococcus lactaris* (Fig. 4A; Table S4; Fig. S8A). Notably, MBL binding to *A. muciniphila* was detected only in IBD-diagnosed donor samples including the 2 samples that lacked *F. prausnitzii* (Fig. 4A; Fig. S7B-C). *F. prausnitzii* levels are reduced in IBD patients (*35*). We reasoned that MBL could exhibit altered or broadened selectivity when its preferred binding partner is largely absent. Additionally, *A. muciniphila* isolates from different individuals are genetically and phenotypically diverse (*36, 37*). Thus, *A. muciniphila* strains associated with disease may have an altered glycan display that leads to differential MBL binding.

MBL and hItln1 bound a similar absolute proportion of cells in samples, but the taxa bound by hItln1 and MBL had little overlap. While MBL preferred *F. prausnitzii*, hItln1-bound fractions consisted of more diverse populations (Fig. S6; Fig. S8B; Table S4). No single species accounted for >15% of the average % relative abundance in hItln1-bound fractions (Fig. 4E; Fig. S6; Fig. S8B; Table S4), and the targeted species were not found in most of the enriched fractions. Nine species were found in five or more hItln1-bound fractions; however, the P_R values for these species varied across samples indicating that enrichment by hItln1 is donor dependent

(Fig. 4F; Fig. S8B). Four species – *A. muciniphila*, *Bifidobacterium longum*, *Ruthenibacterium lactatiformans* and *Coprococcus comes* – had an average positive P_R across all samples (Fig. 4F). These four species each made up less than 2% of the input across all samples and were not detected in the input fractions of most donor samples (Fig. 4G). These findings indicate that hItln1 binds to low-abundance species within the human microbiome, while MBL prefers *F. prausnitzii*, a common and prevalent commensal.

To compare Lectin-Seq to *in vitro* strain binding, we tested MBL and hItln1 binding to select isolates of highly enriched species. MBL bound all tested strains of *A. muciniphila* and *F. prausnitzii* supporting the robust enrichment of the species detected in human samples (Fig. 5A). We also verified that MBL and hItln1 did not bind isolates of species that were depleted from the respective lectin-bound fractions in stool homogenate (Fig. S9). Intriguingly, however, we observed some strain-specific interactions. For example, MBL did not bind any of the tested isolates of *R. lactaris* (Fig. 5A) despite its ability to enrich for this species from human samples. This discrepancy may be due to differences between the *R. lactaris* glycan displays in culture and *in vivo*. Alternately, interactions between *R. lactaris* and MBL may require unknown factors present in stool homogenate that are not present in culture such as bacteria-associated dietary polysaccharides or host immune factors. Lectin strain specificity was even more pronounced for hItln1, which bound 2/3 isolates of *B. longum*, 1/2 isolates of *A. muciniphila*, and no isolates of *C. comes* (Fig. 5B). Because strain identity varies across individual microbiotas (*38*), the donor-dependent enrichment of these species by hItln1 is likely due to strain-specific lectin interactions. These findings highlight the importance of evaluating lectin binding to endogenous bacterial populations. Our data support our findings that MBL binds *F. prausnitzii* and *A. muciniphila* in human samples and provide a mechanistic explanation for the donor-dependent interaction profile of hItln1.

To identify the molecular targets of MBL on the surface of microbial isolates we profiled the glycan displays of isolates of *F. prausnitzii* and *A.muciniphila* isolates using plant-derived lectins with known glycan specificities. Many of the plant lectins showed little ability to bind to isolates enriched by the human lectins. Still, *F. prausnitzii* was robustly bound by concanavalin A (ConA) and wheat germ agglutinin (WGA) (Fig. S10A; Table S7) while *A. muciniphila* was bound by ConA (Fig. S10B; Table S7). The known glycan specificity of ConA is for mannose and glucose while WGA has specificity for N-acetylglucosamine (Table S7). Because MBL binds glycans possessing mannose and N-acetylglucosamine residues, we tested the ability of ConA and WGA to inhibit MBL binding to *F. prausnitzii* (Fig. S10C-D). The plant lectins were effective competitors, suggesting that the human lectin binds the same *F. prausnitzii* glycans. This finding provides a molecular basis for MBL binding specificity in native microbial communities.

Discussion

Historically, the physiological roles of soluble lectins are ascribed to pathogen recognition and clearance (*6*), but emerging data suggest a role for murine lectins in regulating gut microbiota (*9-12*). Whether the glycan-dependent interactomes of human lectins encompass fungal species in the native mycobiome is not clear. We did not detect substantial levels of fungal DNA in our samples (Table S4); however, fungi and bacteria may compete for lectin interactions *in vivo*. We did, however, find that human lectins bind selectively to distinct bacterial species in native communities. Lectin-Seq showed MBL robustly binds *F. prausnitzii*, an abundant member of the gut microbiome, and to a lesser degree *A. muciniphila* and *R. lactaris*. Such specificity suggests MBL could be co-opted as a tool to rapidly quantify the abundance of these species in uncharacterized stool samples. The specificity of MBL binding to

mutualist and commensal species contrasts with previous data indicating that MBL exhibits relatively indiscriminate binding to a broad range of pathogenic microbes (*39*).

The specificity of MBL binding to host-resident microbes suggests its biological functions go beyond pathogen surveillance. MBL is expressed at low levels in the intestine (*27*). The protein could specifically bind to a proportion of abundant commensals such as *F. prausnitzii* to limit their growth and allow for propagation of lower-abundance species. *Akkermansia* levels are decreased in MBL null mice (*12*), but it is unclear whether this decrease is due to direct interactions with murine MBL or if this finding translates to humans. Further mechanistic work is needed to determine the effect of MBL binding on the growth and colonization of these various microbial binding partners in the human gut. In the blood, MBL binding to pathogens results in their clearance (*24*); therefore, in healthy individuals MBL may be poised to eliminate specific gut-resident microbes that breach epithelial barriers and reach the blood. Conversely, in patients diagnosed with IBD or colorectal cancer (CRC) a reduction in barrier integrity can lead to blood, and therefore high levels of MBL, entering different regions of the gut. Indeed, *F. prausnitzii* levels are broadly reduced in patients with IBD (*35*) and, more specifically, in CRC patients that report blood in their stool (*40*). The binding of MBL to *F. prausnitzii* is consistent with these observations.

Lectin-Seq revealed that hItln1 exhibits donor-dependent binding to a broad group of low abundance microbes. hItln1-bound microbes are highly diverse: the population includes Gram-positive and -negative species capable of critical metabolic activities such as short-chain fatty acid production and mucin degradation. Murine Itln1 binds to *A. muciniphila* in mouse stool samples (*41*); our findings show that hItln1 also binds *A. muciniphila* in select human samples. The implications of hItln1 binding to these gut-resident species are unclear. The interaction of hItln1 with select pathogens activates macrophage- and neutrophil-mediated killing (*17, 18, 42*);

however, hItln1-mediated neutrophil activation requires serum components suggesting the bactericidal functions of hItln1 may be limited to the blood. Unlike some intestinal lectins (*11*), hItln1 has no known microbial toxicity and, unlike MBL, lacks canonical domains for complement recruitment (*14*). Alternatively, hItln1 is reported to suppress lipopolysaccharide-induced macrophage activation (*43, 44*), suggesting that under specific conditions hItln1 could play a protective role to shield microbes from macrophage killing. Thus, the function of hItln1 in innate immunity appears to depend on context.

Our data provide insight into the interplay of lectin recognition and microbial glycans. A major finding from our study is that soluble human lectins have strikingly disparate microbial interaction profiles. MBL is highly specific for a prevalent human gut commensal, while hItln1 binds a diverse group of low-abundance species. Further, the orthogonal glycan specificities of these lectins reflect the importance of microbial glycans for species-specific host-microbe interactions. Still unclear is whether MBL and hItln1 have evolved to recognize ligands differentially displayed across the microbiota, or if specific members of the microbiota have evolved mechanisms allowing them to adjust their glycan displays to engage or evade these lectins. Future efforts to identify the microbial genetic determinants of lectin binding will inform the mechanistic basis and evolutionary dynamics of these host-microbe interactions. Our data highlight the utility of Lectin-Seq for uncovering lectin specificity and the need to broadly characterize the interactomes of soluble lectins in native microbial communities.

Materials and Methods

Protein expression, purification and Western blotting

Cloning of full-length N-terminal strepII-tagged hItln1 into the pcDNA4/myc-HisA vector backbone (Life Technologies) was described previously (*14*). Human MBL (*MBL2*, NM_000242) gBlock DNA Fragment (Integrated DNA Technologies) was Gibson ligated into a

linearized pcDNA4 plasmid (primers REV (5'-GGTGAAGCTTAAGTTTAAACG-3') and FWD (5'-TGAGGATCCACTAGTCCAGTG-3')). StrepII tag (5'-TGGAGCCATCCGCAGTTTGAAAAG-3') was inserted C-terminal of amino acid 20 into pcDNA4-hMBL2 using inverse PCR mutagenesis using FWD primer (5'-TGGAGCCATCCGCAGTTTGAAAAGGAAACTGTGACCTGTGAGG-3') and REV primer (5'- TTCTGAGTAAGACGCTGCC-3'). Correct insertion was verified by DNA sequencing (Quintara Biosciences).

HItln1 and MBL were each expressed by transient transfection of suspension-adapted HEK 293T cells. Cells were transfected at 1.8 x 10^6 cells/mL in growth medium (DMEM (Thermo Fisher, cat. no. 11995) supplemented with 10% heat-inactivated fetal bovine serum (FBS), 50 U/mL penicillin-streptomycin, 4 mM L-glutamine, and 1X non-essential amino acids) using lipofectamine 2000 (Thermo Fisher) following the manufacturer's protocol. Six hours after the transfection, culture medium was exchanged to FreeStyle F17 expression medium (Thermo Fisher) supplemented with 50 U/mL penicillin-streptomycin, 4 mM L-glutamine, 1x nonessential amino acids, 0.1% heat-inactivated FBS, and 0.1% pluronic F-68 (Thermo Fisher). Transiently transfected cells were cultured up to 4 days or until viability was below 60%. The conditioned expression medium was then harvested by centrifugation and sterile filtration.

For purification, $CaCl_2$ was added to the harvested conditioned expression medium to a final concentration of 10 mM, avidin (7 mg/mL) was added at 12 µL per mL of expression media (IBA, cat. no. 2-0204-015, per the IBA protocol). Protein was captured onto 2 mL of Strep-Tactin Superflow High-Capacity resin (IBA Lifesciences, cat. no. 2-1208-002) equilibrated with HEPES-Ca buffer (20 mM HEPES pH 7.4, 150 mM NaCl, 10 mM $CaCl_2$). The resin was then washed with HEPES-EDTA buffer (20 mM HEPES pH 7.4, 150 mM NaCl, 1 mM EDTA), and eluted with 5 mM *d*-desthiobiotin (Sigma) in HEPES-EDTA buffer. StrepII-tagged hItln1 was

concentrated with a 30,000-MWCO Amicon Ultra centrifugal filter. StrepII-tagged MBL was concentrated with a 10,000-MWCO Vivaspin 6 centrifugal filter (GE). All proteins were buffer exchanged to HEPES-EDTA buffer for storage. Protein concentrations were determined by absorbance at 280 nm. Extinction coefficients and molecular weights were calculated for the mature trimeric product of each protein (without the signal peptide) using the ProtParam tool (web.expasy.org/protparam). StrepII-tagged hItln1 had a calculated $\varepsilon = 239{,}775\ cm^{-1}\ M^{-1}$ and an estimated molecular mass of 102,024 Da. StrepII-tagged MBL had a calculated $\varepsilon = 71{,}595\ cm^{-1}\ M^{-1}$ and an estimated molecular mass of 75,570 Da.

Recombinant hItln1 and MBL were characterized by western blotting using monoclonal mouse anti-MBL2 antibody (3E7; ThermoFisher Scientific MA1-40145; 1:50) and polyclonal rabbit anti-hItln1 antibody (Proteintech 11770-1-AP; 1:2000).

Culturing of microbial isolates

Bacterial isolates along with their respective media used in this study are detailed in Table S1 and Table S6. All isolates were struck out from frozen stock onto solid medium in an anaerobic chamber and incubated anaerobically at 37°C for 24-72 hours (isolate-dependent). Liquid Mega Medium (isolates in Table S1) was prepared and reduced in a Coy Laboratory anaerobic chamber (5% H_2, 20% CO_2, 75% N_2) as previously described (*45*). Bacteria in Table S6 were grown in CHG medium (*46*) (Brain Heart Infusion (37 g L−1, Sigma-Aldrich) supplemented with 5% sterile-filtered fetal bovine serum (Sigma-Aldrich), 1% vitamin K1-hemin solution (BD Biosciences), 1% trace mineral supplement (ATCC), 1% trace vitamin supplement (ATCC), 1 g L−1 D-(+)-cellobiose (Sigma-Aldrich), 1 g L−1 D-(+)-maltose (Sigma-Aldrich), 1 g L−1 D-(+)-fructose (Sigma-Aldrich) and 0.5 g L−1 L-cysteine (Sigma-Aldrich) or YCFAC medium (Yeast Casitone Fatty Acids Agar with Carbohydrates, Anaerobe Systems). Liquid cultures were

established for each isolate through the inoculation of a single colony into 5-10 mL of media. Upon the observation of turbid growth (16-72 hours), liquid cultures were combined with a 1X phosphate buffered saline (PBS) + 40% glycerol + 0.001% L-cysteine solution at a 1:1 ratio, aliquoted into a series of cryovials, and stored at -80°C prior to flow cytometry. A portion of each culture was subjected to 16S rDNA V1-V9 PCR amplification, spin column purification, and Sanger sequencing, with taxonomic verification via standard nucleotide BLAST via blastn suite software (NIH, National Library of Medicine, https://blast.ncbi.nlm.nih.gov/Blast.cgi).

Flow cytometry of microbial isolates

All buffers were sterile filtered before use and all centrifugation steps were performed at 5000 relative centrifugal force (RCF) at 4°C. Microbial isolates were screened for viability by propidium iodide staining by flow cytometry prior to lectin binding. We observed differences in binding to viable and unviable cells; therefore, only viable isolates were used for validation. Microbial isolates washed 2X with 2mL PBS-BSA-T (PBS pH 7.4, Gibco, 0.1% (w/v) BSA (US Biological; A1311), 0.05% (v/v) Tween-20 (Sigma), pelleted, and resuspended in PBS-BSA-T. Staining was performed at OD_{600} of 0.2 for all samples. Staining solutions were HEPES-Ca-BSA-T with SYTO BC (1:1000, Thermo Fisher Scientific) and StrepMAB classic DY649-conjugate (1:150, IBA Lifesciences) for the unstained samples. All lectin-stained Ca^{2+} samples were stained as follows: HEPES-Ca-BSA-T, SytoBC (1:1000; Fig. 5, Fig. S5), StrepMAB classic Oyster 645 (1:250, Fig. 1, Table S1) or StrepMAB classic DY649-conjugate (1:250; Fig. 5, Fig. S5), 20 µg/mL recombinant StrepII-tagged lectin. For the lectin-stained EDTA control samples, the staining conditions were as follows: HEPES-EDTA-BSA-T (20 mM HEPES pH 7.4, 150 mM NaCl, 1 mM EDTA, 0.1% BSA, 0.05% Tween-20), SytoBC (1:1000), StrepMAB classic DY649-conjugate (1:250), and 20 µg/mL recombinant StrepII-tagged lectin. Staining was

performed at 4 °C for one hour before being diluted 4X without washing and analyzed on a BD Accuri C6 flow cytometer (Fig. 1, Table S1) or ThermoFisher Scientific Attune flow cytometer (Fig. 5, Fig. S6).

For plant lectin staining microbial isolates were prepared as described above prior to staining. Biotinylated plant lectins were purchased from Vector Laboratories. All plant lectin-stained samples were stained as follows: HEPES-Ca-BSA-T, SytoBC (1:1000), Strep-Tactin XT DY649 (1:250), 20 μg/mL biotinylated plant lectin. Staining was performed at 4 °C for one hour before being diluted 4X without washing and analyzed on a ThermoFisher Scientific Attune flow cytometer.

For competition assays microbial isolates were prepared as described above prior to staining. Unlabeled plant lectins were purchased from Vector Laboratories. All competition assay samples were pre-incubated with indicated concentrations of unlabeled plant lectins at 4 °C for one hour. Samples were then stained as follows: HEPES-Ca-BSA-T, SytoBC (1:1000), StrepMAB classic DY649-conjugate (1:250), 20 μg/mL StrepII-tagged MBL. Staining was performed at 4 °C for one hour before being diluted 4X without washing and analyzed on a ThermoFisher Scientific Attune flow cytometer.

hItln1 binding to synthetic mixed community

Strains of bacteria were prepared as described above. Cell density was quantified on a BD Accuri C6 flow cytometer and equal numbers of cells from each species were combined into a single sample at a final cell concentration of 5e7 to 1e8 cells/mL. Indicated amounts of hItln1 were added per 1e6 cells in the final sample (final concentrations ranged from 5-50 μg/mL). Cells were stained and analyzed as described above.

Direct labeling of proteins with fluorophores

Recombinant StrepII-tagged hItln1 and MBL were directly conjugated with fluorophores using NHS-ester conjugation chemistry. HItln1 was labeled with Alexa Fluor 647 NHS Ester (Succinimidyl Ester) (ThermoFisher Scientific) and MBL was labeled with Alexa Fluor 555 NHS Ester (Succinimidyl Ester) (ThermoFisher Scientific) following manufacturers protocol as follows: proteins were labeled in storage buffer (HEPES-EDTA, pH 7.4 as described above) by the addition of dye dissolved in dimethyl sulfoxide (DMSO) at a ratio of 1:4 (w:w, dye:protein), and incubation for 1 hour at room temperature with mixing. Unreacted dye was removed by desalting using a Zeba 2 mL 7K MWCO Spin Desalting Column (ThermoFisher Scientific) following manufacturer protocol. Molar ratio of fluorophore:protein was determined from UV-Vis absorbance spectrum using the extinction coefficients: ε Alexa Fluor 555 = 155,000 cm^{-1} M^{-1}, ε Alexa Fluor 647 = 270,000 cm^{-1} M^{-1}.

Glycan array analysis

Microbial Glycan Microarrays (MGM) were synthesized as previously described (*14, 47*) and are commercially available from the National Center for Functional Glycomics (NCFG). For each lectin an MGM was thawed at room temperature for 30 minutes. The slide was placed in a slide holder tube and soaked in wash buffer (20 mM HEPES pH 7.5, 150 mM NaCl) for 10 minutes. The slide was placed onto a raised slide holder platform in a humidification chamber and a solution of StrepII-tagged lectin at a concentration of 10 μg/mL in binding buffer (20 mM HEPES pH 7.5, 150 mM NaCl, 10 mM $CaCl_2$, 0.1% BSA, 0.1% Tween-20). The slide was incubated with gentle rocking at room temperature for 1 hour. The slide was then washed with binding buffer, wash buffer and ddH_2O (4 times each). The slide was placed back into the humidification chamber and incubated with DY549-conjugated anti-Strep Mab at 4 μg/mL in

binding buffer at room temperature for 1 hour. The slide was washed again with binding buffer, wash buffer and ddH_2O (4 times each). The slide was dried with a slide spinner and scanned using a Genepix4000 (Molecular Devices) using the 532 nm laser. Raw data was averaged across technical replicates and plotted against sample ID numbers.

Approval for human sample research

Human stool samples were obtained from the Prospective Registry in IBD Study at MGH (PRISM) cohort, which was reviewed and approved by the Partners Human Research Committee (ref. 2004-P-001067). Stool samples from healthy subjects were obtained under protocol approved by the institutional review board at MIT (IRB protocol ID no. 1510271631). Participants under both protocols provided informed consent and all experiments adhered to the regulations of the review boards.

Preparation of human stool samples

Healthy human stool samples from IRB protocol ID no. 1510271631 were prepared was as follows: healthy subjects stool samples were brought into the anaerobic chamber within 2 hours of donation. Samples were homogenized using 1X PBS (pH 7.4), 0.1% L-cysteine at a ratio of 1 g stool:2.5 mL PBS. Glycerol (25% in 1X PBS, 0.1% L-cysteine) was added to the homogenate to a concentration of 12.5%, giving a final solution of 1g stool in 5mL 1X PBS, 0.1% L-cysteine, and 12.5% glycerol. The homogenate was removed from the anaerobic chamber and stored at -80°C prior to FACS analysis.

Fresh stool samples from adult donors with inflammatory bowel disease from the PRISM cohort were collected in anaerobic transport medium (Anaerobic Systems, AS-690), mailed at ambient temperature, and processed anaerobically within 24-72 hours of collection. In the

anaerobic chamber, samples were decanted into sterile gentleMACS C tubes (Miltenyi Biotec, 130-093-237) and topped up to a total volume of 10 mL using 1X PBS + 40% glycerol + 0.001% L-cysteine solution, respectively. Stool was homogenized via gentleMACS Dissociator (Miltenyi Biotec, 130-093-235) for 3 cycles of 61 s on the "intestine" setting, aliquoted into a series of 2.0 mL cryovials (Corning, 430659), and stored at -80°C prior to FACS analysis.

Flow cytometry and FACS of donor stool samples

All buffers were sterile filtered before use and all centrifugation steps were performed at 5000 RCF at 4°C. Stool homogenate was thawed on ice and 200ul of homogenate was washed 2X with 2mL PBS-BSA-T (PBS pH 7.4, Gibco, 0.1% (w/v) BSA (US Biological; A1311), 0.05% (v/v) Tween-20 (Sigma), pelleted, and resuspended in PBS-BSA-T. The material was then passed through a 35 µm cell strainer cap (Falcon), pelleted, and resuspended in 2 mL HEPES-Ca-BSA-T (20 mM HEPES pH 7.4, 150 mM NaCl, 10 mM $CaCl_2$, 0.1% BSA, 0.05% tween-20). A 5 µL sample of the bacterial suspension was pelleted and frozen as the input sample for metagenomic sequencing. Staining was performed at OD_{600} of 0.2 for all samples. Staining solutions were HEPES-Ca-BSA-T with SYTO BC (1:1000, Thermo Fisher Scientific) and StrepMAB classic DY649-conjugate (1:250, IBA Lifesciences) for the unstained samples. All lectin-stained Ca^{2+} samples were stained as follows: HEPES-Ca-BSA-T, SytoBC (1:1000), StrepMAB classic DY649-conjugate (1:250), and 20 µg/mL recombinant StrepII-tagged lectin unless indicated otherwise. For the lectin-stained EDTA control samples, the staining conditions were as follows: HEPES-EDTA-BSA-T (20 mM HEPES pH 7.4, 150 mM NaCl, 1 mM EDTA, 0.1% BSA, 0.05% Tween-20), SytoBC (1:1000), StrepMAB classic DY649-conjugate (1:250), and 20 µg/mL recombinant StrepII-tagged lectin unless indicated otherwise. For the lectin-stained mannan and glycerol control samples the staining conditions were as follows: HEPES-

Ca-BSA-T, indicated concentrations of mannan (Millipore Sigma M7504) or glycerol, SytoBC (1:1000), StrepMAB classic DY649-conjugate (1:250), and 20 μg/mL recombinant StrepII-tagged lectin. For mock stool homogenization samples were stained with lectin in HEPES-Ca-BSA-T as described above without SYTOBC and StrepMAB classic DY649-conjugate. Samples were then washed 1X with 1X PBS 12.5% glycerol and 3X with 1X PBS. Washed samples were then stained with SytoBC and StrepMAB classic DY649-conjugate as described above. Staining was performed at 4°C for four hours before being diluted 10X without washing and analyzed on a BD LSRII HTS flow cytometer with BD FACSDiva software or an Attune Flow Cytometer (ThermoFisher Scientific), or diluted 6X without washing and sorted by FACS on a FACS Aria contained in a biosafety cabinet, with BD FACSDiva software. Stained samples were screened for viability by propidium iodide staining prior to lectin binding and sorting. Under our staining conditions lectin binding did not alter cell viability (Fig. S11). Cells were gated by forward scatter, side scatter, and SYTO BC staining, and sorted into lectin-negative or lectin-positive fractions. For metagenomics, 1.5×10^6 cells were collected for the lectin-negative and -positive samples. Sorted cells were centrifuged at 7,000 RCF at 4°C for 5 minutes, supernatant was removed, and the cell pellet was stored at -20°C prior to nucleic acid extraction.

Stool samples were stained for endogenous hItln1 and MBL using using monoclonal mouse anti-MBL2 antibody (3E7; ThermoFisher Scientific MA1-40145; 1:50) and polyclonal rabbit anti-hItln1 antibody (Proteintech 11770-1-AP; 1:450). Primary antibodies were detected using goat anti-Mouse AF555 (ThermoFisher Scientific A-21422; 1:1000) and goat anti-Rabbit AF555 (ThermoFisher Scientific A-31572; 1:1000). Stool samples were prepared as described above and stained in HEPES-Ca-BSA-T with SYTO BC (1:1000, ThermoFisher Scientific) for 1 hour at 4°C and analyzed on an Attune Flow Cytometer (ThermoFisher Scientific).

Flow cytometry on stool samples was performed at the The Swanson Biotechnology Center Flow Cytometry Facility housed in the Koch Institute (Massachusetts Institute of Technology, Cambridge, MA).

5 *Nucleic acid extraction*

Cell pellets were lysed by the HotSHOT lysis method (*48, 49*). HotSHOT lysis offers advantages for workflows that deal with low volumes and cell counts; however, this method is inefficient at lysing certain classes of microbes. As a result select species may be underrepresented across all samples. Notably, this should not impact comparisons between Lectin+ and Lectin- fractions.

10 Briefly, cell pellets were lysed by addition of 50 μL HotSHOT Lysis buffer (25 mM NaOH, 0.2 mM EDTA, pH 12), and heating to 95°C for 10 minutes followed by addition of equal volume HotSHOT neutralization buffer (40 mM Tris-HCl, pH 5) and vortexed to combine. Lysed samples were centrifuged at 3000 RCF for 10 minutes to pellet debris and transferred to 96 well plates. The genomic DNA was then purified by AMPURE bead cleanup as follows: 90 μL beads

15 was added to 100 μL DNA and incubated for 13 minutes at room temperature. Beads were separated on a magnet for 2 minutes and supernatant removed. Beads were washed 2X with 200 μL EtOH and air dried for 20 minutes while still on the magnet. The elution was performed by resuspending the beads thoroughly in 30 μL H_2O and incubation for 7 minutes at room temperature. Beads were separated on a magnet and 27 μL eluted DNA was removed to a sterile

20 plate.

Metagenomics Library Construction and Sequencing

1 μL of purified DNA was directly used as input into a miniaturized version of the Nextera-XT Library Preparation Kit (Illumina Inc.). All reactions were scaled to one-fourth their original

volumes. Libraries were constructed according to the manufacturer's instructions with several modifications to accommodate low DNA concentrations. The amplicon tagmentation mix (ATM) was diluted 1:10 in tagmentation DNA buffer (TD) to reduce the tagmentase:DNA ratio. Tagmentation time was also reduced from 5 minutes to 1 minute. Both modifications were implemented to boost the insert size thereby reducing read overlap and allowing for sampling of a larger proportion of the nucleotide sequence space. Lastly, the number of cycles in the library amplification PCR was increased from 12 to 20 to generate sufficient product for sequencing. The concentrations of sample libraries were normalized, and the libraries were pooled at equimolar concentrations and sequenced on a HiSeq 2500 at 200 cycles for 2x100 paired-end reads.

Metagenomic Profiling and Downstream Analysis

Raw sequencing reads were first processed through CutAdapt (version 1.7.1) (*50*) and Trimmomatic (*51*) (version 0.3.3) to remove Nextera adapters, low quality bases, and low quality reads. Trimmed reads were then filtered for human contamination (Hg19) with KneadData (version 0.5.1). These filtered reads were then run through Metaphlan2 (version 2.6.0) for taxonomic profiling (*33, 52*). Relative taxonomic abundances from Metaphlan2 were imported into the phyloseq package (version 1.30.0) for further refinement and visualization.

We categorized microbial species that were found in buffer controls as contaminants (most notably, the skin-resident microbe *Cutibactierum acnes*) and excluded these species from downstream analyses. Relative taxonomic abundances were used to calculate enrichment scores (Probability Ratios; P_R) in R using the IgAScores package (version 0.1.2) (*34*). To calculate probability ratio enrichments in the case of a species present in the lectin-bound fraction but undetected in the input, we added a pseudo-count of 0.00001 for the abundance of that species in

the input sample. Data were further processed using TidyR (version 1.1.4) and visualized by ggplot2 (version 3.3.5).

References and Notes

1. P. J. Turnbaugh *et al.*, The Human Microbiome Project. *Nature* **449**, 804-810 (2007).
2. A. Varki, *Essentials of glycobiology*. (Cold Spring Harbor Laboratory Press, Cold Spring Harbor, New York, ed. Third edition., 2017), pp. xxix, 823 pages.
3. H. L. Tytgat, S. Lebeer, The sweet tooth of bacteria: common themes in bacterial glycoconjugates. *Microbiol Mol Biol Rev* **78**, 372-417 (2014).
4. H. L. a. N. Sharon, Lectins: Carbohydrate-Specific Proteins That Mediate Cellular Recognition. *Chemical Reviews* **98**, 637-674 (1998).
5. W. I. Weis, K. Drickamer, W. A. Hendrickson, Structure of a C-type mannose-binding protein complexed with an oligosaccharide. *Nature* **360**, 127-134 (1992).
6. D. A. Wesener, A. Dugan, L. L. Kiessling, Recognition of microbial glycans by soluble human lectins. *Current Opinion in Structural Biology* **44**, 168-178 (2017).
7. T. Fujita, Evolution of the lectin–complement pathway and its role in innate immunity. *Nature Reviews Immunology* **2**, 346-353 (2002).
8. S. R. Stowell *et al.*, Innate immune lectins kill bacteria expressing blood group antigen. *Nature Medicine* **16**, 295-301 (2010).
9. J. H. Bergstrom *et al.*, Gram-positive bacteria are held at a distance in the colon mucus by the lectin-like protein ZG16. *Proc Natl Acad Sci U S A* **113**, 13833-13838 (2016).
10. H. Sarashina-Kida *et al.*, Gallbladder-derived surfactant protein D regulates gut commensal bacteria for maintaining intestinal homeostasis. *Proc Natl Acad Sci U S A* **114**, 10178-10183 (2017).

11. S. Vaishnava *et al.*, The Antibacterial Lectin RegIIIγ Promotes the Spatial Segregation of Microbiota and Host in the Intestine. *Science* **334**, 255 (2011).

12. M. Wu *et al.*, The responses of the gut microbiota to MBL deficiency. *Mol Immunol* **122**, 99-108 (2020).

13. W. I. Weis, K. Drickamer, Structural basis of lectin-carbohydrate recognition. *Annual Review of Biochemistry* **65**, 441-473 (1996).

14. D. A. Wesener *et al.*, Recognition of microbial glycans by human intelectin-1. *Nature Structural & Molecular Biology* **22**, 603-610 (2015).

15. J. Gao, D. Liu, Z. Wang, Screening lectin-binding specificity of bacterium by lectin microarray with gold nanoparticle probes. *Anal Chem* **82**, 9240-9247 (2010).

16. K. L. Hsu, K. T. Pilobello, L. K. Mahal, Analyzing the dynamic bacterial glycome with a lectin microarray approach. *Nat Chem Biol* **2**, 153-157 (2006).

17. S. Andresen *et al.*, Human Intelectin-1 Promotes Cellular Attachment and Neutrophil Killing of Streptococcus pneumoniae in a Serotype-Dependent Manner. *Infect Immun*, e0068221 (2022).

18. M. Sigal *et al.*, R-spondin-3 induces secretory, antimicrobial Lgr5(+) cells in the stomach. *Nat Cell Biol* **21**, 812-823 (2019).

19. S. Tsuji *et al.*, Human Intelectin Is a Novel Soluble Lectin That Recognizes Galactofuranose in Carbohydrate Chains of Bacterial Cell Wall. *Journal of Biological Chemistry* **276**, 23456-23463 (2001).

20. S. R. Gill *et al.*, Metagenomic analysis of the human distal gut microbiome. *Science* **312**, 1355-1359 (2006).

21. C. M. McMahon *et al.*, Stereoelectronic Effects Impact Glycan Recognition. *Journal of the American Chemical Society* **142**, 2386-2395 (2020).

22. J. C. Barrett *et al.*, Genome-wide association defines more than 30 distinct susceptibility loci for Crohn's disease. *Nature Genetics* **40**, 955-962 (2008).

23. A. D. Pemberton, M. J. Rose-Zerilli, J. W. Holloway, R. D. Gray, S. T. Holgate, A single-nucleotide polymorphism in intelectin 1 is associated with increased asthma risk. *Journal of Allergy and Clinical Immunology* **122**, 1033-1034 (2008).

24. R. M. Dommett, N. Klein, M. W. Turner, Mannose-binding lectin in innate immunity: past, present and future. *Tissue Antigens* **68**, 193-209 (2006).

25. O. Neth *et al.*, Mannose-Binding Lectin Binds to a Range of Clinically Relevant Microorganisms and Promotes Complement Deposition. *Infection and Immunity* **68**, 688 (2000).

26. W. I. Weis, K. Drickamer, Trimeric structure of a C-type mannose-binding protein. *Structure* **2**, 1227-1240 (1994).

27. J. Seyfarth, P. Garred, H. O. Madsen, Extra-hepatic transcription of the human mannose-binding lectin gene (mbl2) and the MBL-associated serine protease 1–3 genes. *Molecular Immunology* **43**, 962-971 (2006).

28. K. Drickamer, M. E. Taylor, Recent insights into structures and functions of C-type lectins in the immune system. *Curr Opin Struct Biol* **34**, 26-34 (2015).

29. W. I. Weis, M. E. Taylor, K. Drickamer, The C-type lectin superfamily in the immune system. *Immunological Reviews* **163**, 19-34 (1998).

30. S. Herget *et al.*, Statistical analysis of the Bacterial Carbohydrate Structure Data Base (BCSDB): characteristics and diversity of bacterial carbohydrates in comparison with mammalian glycans. *BMC Struct Biol* **8**, 35 (2008).

31. L. Oinam, H. Tateno, Glycan Profiling by Sequencing to Uncover Multicellular Communication: Launching Glycobiology in Single Cells and Microbiomes. *Front Cell Dev Biol* **10**, 919168 (2022).

32. A. Vich Vila *et al.*, Gut microbiota composition and functional changes in inflammatory bowel disease and irritable bowel syndrome. *Science Translational Medicine* **10**, eaap8914 (2018).

33. D. T. Truong *et al.*, MetaPhlAn2 for enhanced metagenomic taxonomic profiling. *Nature Methods* **12**, 902-903 (2015).

34. M. A. Jackson *et al.*, Accurate identification and quantification of commensal microbiota bound by host immunoglobulins. *Microbiome* **9**, 33 (2021).

35. Y. Cao, J. Shen, Z. H. Ran, Association between Faecalibacterium prausnitzii Reduction and Inflammatory Bowel Disease: A Meta-Analysis and Systematic Review of the Literature. *Gastroenterol Res Pract* **2014**, 872725 (2014).

36. X. Guo *et al.*, Genome sequencing of 39 Akkermansia muciniphila isolates reveals its population structure, genomic and functional diverisity, and global distribution in mammalian gut microbiotas. *BMC Genomics* **18**, 800 (2017).

37. B. Becken *et al.*, Genotypic and Phenotypic Diversity among Human Isolates of Akkermansia muciniphila. *mBio* **12**, (2021).

38. Y. Yan, L. H. Nguyen, E. A. Franzosa, C. Huttenhower, Strain-level epidemiology of microbial communities and the human microbiome. *Genome Med* **12**, 71 (2020).

39. B. T. Seiler *et al.*, Broad-spectrum capture of clinical pathogens using engineered Fc-mannose-binding lectin enhanced by antibiotic treatment. *F1000Res* **8**, 108 (2019).

40. T. Chenard, M. Malick, J. Dube, E. Masse, The influence of blood on the human gut microbiome. *BMC Microbiol* **20**, 44 (2020).

41. J. D. Matute *et al.*, Intelectin-1 binds and alters the localization of the mucus barrier-modifying bacterium Akkermansia muciniphila. *J Exp Med* **220**, (2023).

42. S. Tsuji *et al.*, Capture of heat-killed Mycobacterium bovis bacillus Calmette-Guérin by intelectin-1 deposited on cell surfaces. *Glycobiology* **19**, 518-526 (2009).

43. H. Kobayashi *et al.*, Intelectin1 ameliorates macrophage activation via inhibiting the nuclear factor kappa B pathway. *Endocr J*, (2021).

44. J. Wang, Y. Gao, F. Lin, K. Han, X. Wang, Omentin-1 attenuates lipopolysaccharide (LPS)-induced U937 macrophages activation by inhibiting the TLR4/MyD88/NF-kappaB signaling. *Arch Biochem Biophys* **679**, 108187 (2020).

45. K. A. Romano, E. I. Vivas, D. Amador-Noguez, F. E. Rey, Intestinal microbiota composition modulates choline bioavailability from diet and accumulation of the proatherogenic metabolite trimethylamine-N-oxide. *mBio* **6**, e02481 (2015).

46. A. B. Hall *et al.*, A novel Ruminococcus gnavus clade enriched in inflammatory bowel disease patients. *Genome Med* **9**, 103 (2017).

47. S. R. Stowell *et al.*, Microbial glycan microarrays define key features of host-microbial interactions. *Nat Chem Biol* **10**, 470-476 (2014).

48. G. E. Truett *et al.*, Preparation of PCR-quality mouse genomic DNA with hot sodium hydroxide and tris (HotSHOT). *Biotechniques* **29**, 52, 54 (2000).

49. J. D. Brewster, G. C. Paoli, DNA extraction protocol for rapid PCR detection of pathogenic bacteria. *Anal Biochem* **442**, 107-109 (2013).

50. M. Martin, Cutadapt removes adapter sequences from high-throughput sequencing reads. *EMBnet.journal; Vol 17, No 1: Next Generation Sequencing Data Analysis*, (2011).

51. A. M. Bolger, M. Lohse, B. Usadel, Trimmomatic: a flexible trimmer for Illumina sequence data. *Bioinformatics* **30**, 2114-2120 (2014).

52. L. J. McIver *et al.*, bioBakery: a meta'omic analysis environment. *Bioinformatics* **34**, 1235-1237 (2017).

Acknowledgements: We would like to thank Luke Besse for project management and the Broad Institute's Microbial 'Omics Core and Genomics Platform for sample processing and sequencing data generation. We also thank Damian Plichta at the Broad Institute for helpful discussions. We are grateful to all study participants who provided samples and to Helena Lau and Kevin Shannon for clinical sample coordination for the PRISM cohort.

Funding:

Center for Microbiome Informatics and Therapeutics (HV, RJX, LLK)

National Institutes of Health grant R01HL148577 (FER)

National Institutes of Health grant R01AI055258 (LLK)

National Institutes of Health grant U01CA231079 (LLK)

Helen Hay Whitney Foundation postdoctoral fellowship (RLM)

NSF GRFP predoctoral fellowship (CRI)

Author contributions:

Conceptualization: CRI, DAW, LLK

Methodology: RLM, CRI, RLW, DS, TG, SR, LTTN, DAW, MH, MW, AD, RK, SG, SHB, CD, GP

Investigation: RLM, CRI, RLW, DS, TG, SR, LTTN, DAW, MH, MW, AD, RK, SG, SHB, CD

Visualization: RLM, CRI, RLW, MW

Funding acquisition: RLM, CRI, FER, HV, RJX, LLK

Project administration: HV, EJA, RJX, LLK

Supervision: HV, EJA, RJX, LLK

Writing – original draft: RLM, CRI, RLW, DS, MH, HV, LLK

Writing – review & editing: RLM, CRI, SHB, LLK

Competing interests: The authors are coinventors on patents and disclosures pertaining to the results presented in the manuscript.

Data and materials availability: Metagenomic sequences are available via Sequence Read Archive (https://www.ncbi.nlm.nih.gov/sra) with BioProject number PRJNA905698.

Supplementary Materials

Figs. S1 to S11

Tables S1 to S8

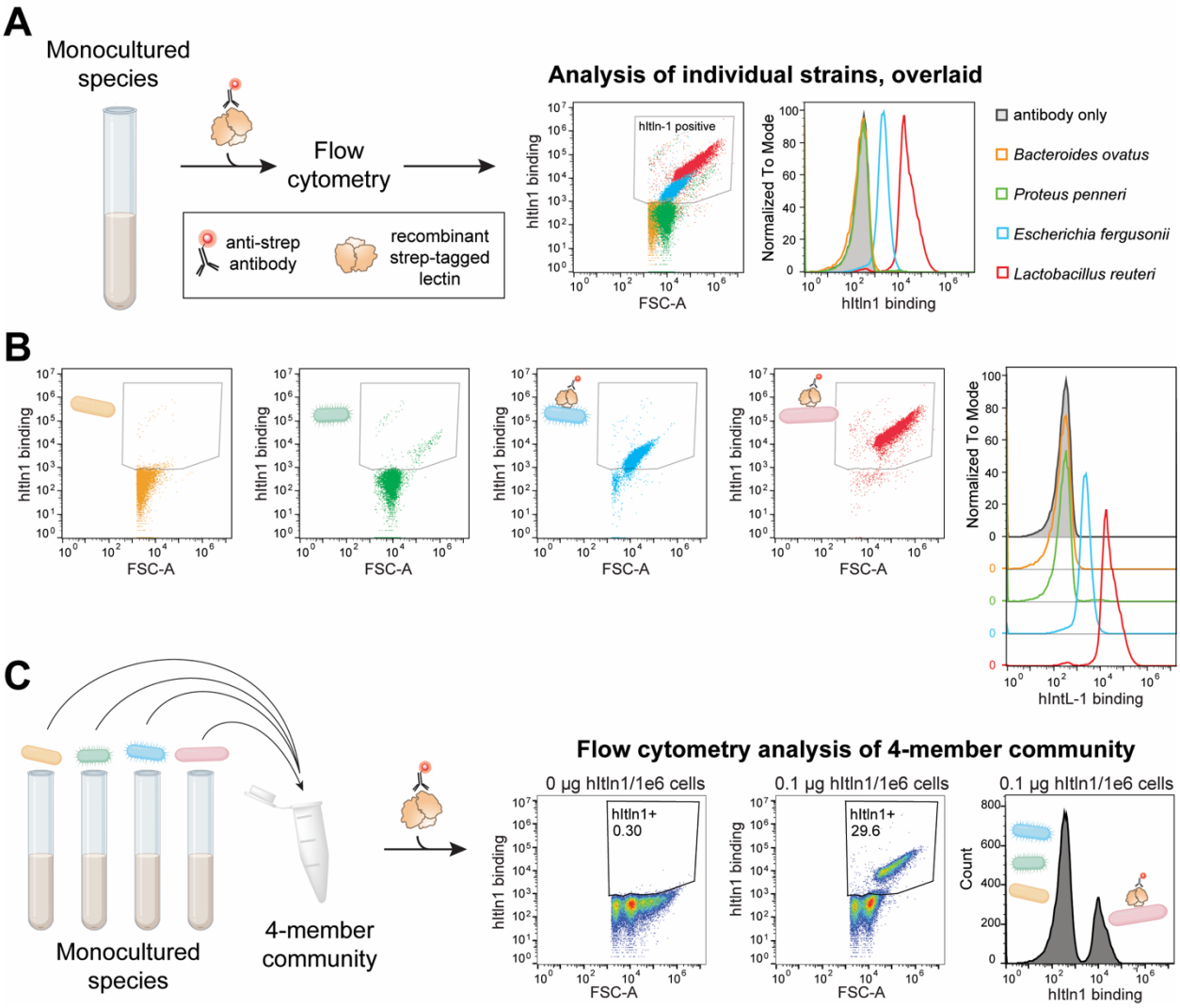

Figure 1. hItln1 binding in a synthetic mixed microbial community. (A) Schematic of flow cytometry-based assay to measure soluble lectin binding to microbial isolates. Overlay of data from 0.1 µg hItln1/1e6 cells condition shown in (B) with the hItln1-positive binding region indicated. **(**B) Flow cytometry analysis of microbial isolates plotted as forward scatter (FSC) against hItln1 binding (anti-Strep Oyster 645). Panels show 0.1 µg hItln1/1e6 cells condition. Staggered histograms of flow cytometry data plot cell count as a percent of the maximum against lectin binding (anti-Strep Oyster 645). Dot plots and histograms are color-coded according to the legend shown in (A). (C) Schematic of flow cytometry-based assay to measure soluble lectin binding to a synthetic mixture of microbial isolates. Flow cytometry analysis of synthetic mixed

microbial community plotted as forward scatter (FSC) against hItln1 binding (anti-Strep Oyster 645). Panels show 0 μg hItln1/1e6 cells and 0.1 μg hItln1/1e6 cells conditions. Histogram of flow cytometry data plots cell count as a percent of the maximum against lectin binding (anti-Strep Oyster 645) for the 0.1 μg hItln1/1e6 cells condition. Data are representative of two independent experiments.

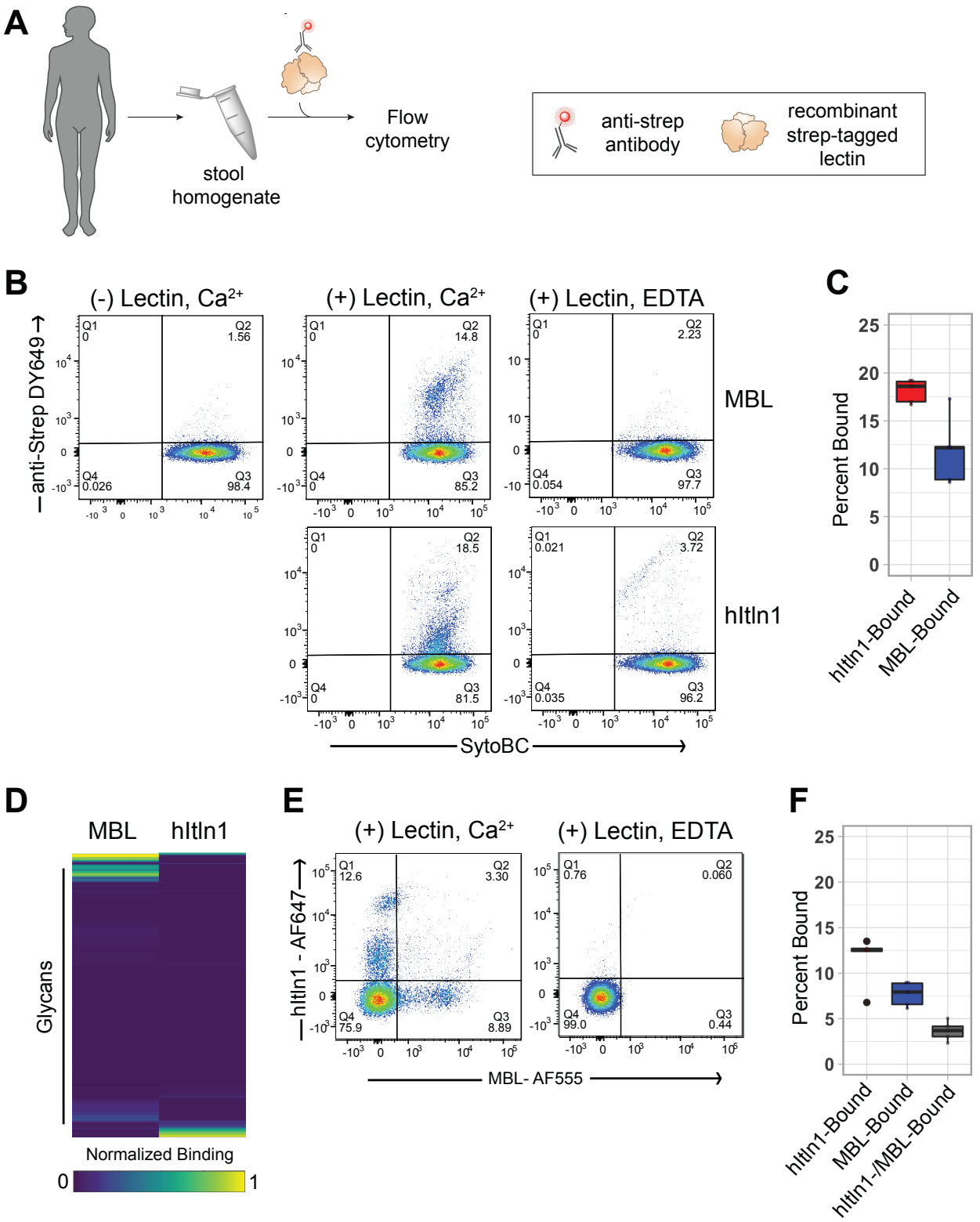
A
stool homogenate
Flow cytometry
anti-strep antibody
recombinant strep-tagged lectin
B
(-) Lectin, Ca2+
(+) Lectin, Ca2+
(+) Lectin, EDTA
anti-Strep DY649
MBL
hItln1
SytoBC
Q1 0
Q2 1.56
Q4 0.026
Q3 98.4
Q2 14.8
Q3 85.2
Q2 2.23
Q4 0.054
Q3 97.7
Q2 18.5
Q3 81.5
Q1 0.021
Q2 3.72
Q4 0.035
Q3 96.2
C
Percent Bound
hItln1-Bound
MBL-Bound
D
MBL
hItln1
Glycans
Normalized Binding
0
1
E
(+) Lectin, Ca2+
(+) Lectin, EDTA
hItln1 - AF647
MBL- AF555
Q1 12.6
Q2 3.30
Q4 75.9
Q3 8.89
Q1 0.76
Q2 0.060
Q4 99.0
Q3 0.44
F
Percent Bound
hItln1-Bound
MBL-Bound
hItln1-/MBL-Bound

Figure 2. MBL and hItln1 binding to microbial populations in human stool samples. (A) Schematic of flow cytometry-based assay to measure soluble lectin binding to stool microbiome. (B) Flow cytometry analysis of healthy human stool plotted as SytoBC against lectin binding (anti-Strep DY649). Panels show no lectin control (column 1), and strep-MBL (top row) or strep-hItln1 (bottom row) binding in the presence of Ca^{2+} (column 2) or EDTA (column 3). (C) Quantification of data shown in A. Percent bound is calculated by determining the percentage of cells that fall in the strep-pos/SytoBC-pos fraction (Q2). Data shown (boxplots represent the mean and standard deviation; reported values are mean and standard error of the mean) are from the (+) strep-hItln1/Ca^{2+} (red; n=5; 18.1 +/- 0.5 %) and (+) strep-MBL/Ca^{2+} (blue; n=5; 11.9 +/- 1.6%) samples. (D) Heatmap depicting normalized binding of MBL and hItln1 to microbial glycan array. Each row represents binding to a single glycan (mean of three spots). Rows were grouped by hierarchical clustering (Euclidean). (E) Flow cytometry analysis of the stool microbiome to determine differential hItln1 and MBL binding. Flow cytometry data is plotted as hItln1-binding (AF-647) against MBL-binding (AF-555). Panels show lectin-binding in the presence of (+) lectin/Ca^{2+} (panel 1) or (+) lectin/EDTA (panel 2). (F) Quantification of data (boxplots represent the mean and standard deviation; reported values are mean and standard error of the mean) shown in E, panel 2. Percent bound is calculated by determining the percentage of cells that fall in the hItln1-pos/MBL-neg (red; n=5; 11.6 +/- 1.2%), hItln1-neg/MBL-pos (blue; n=5; 7.7 +/- 0.6%) and hItln1-pos/MBL-pos fractions (dark grey; n=5; 3.6 +/- 0.5%).

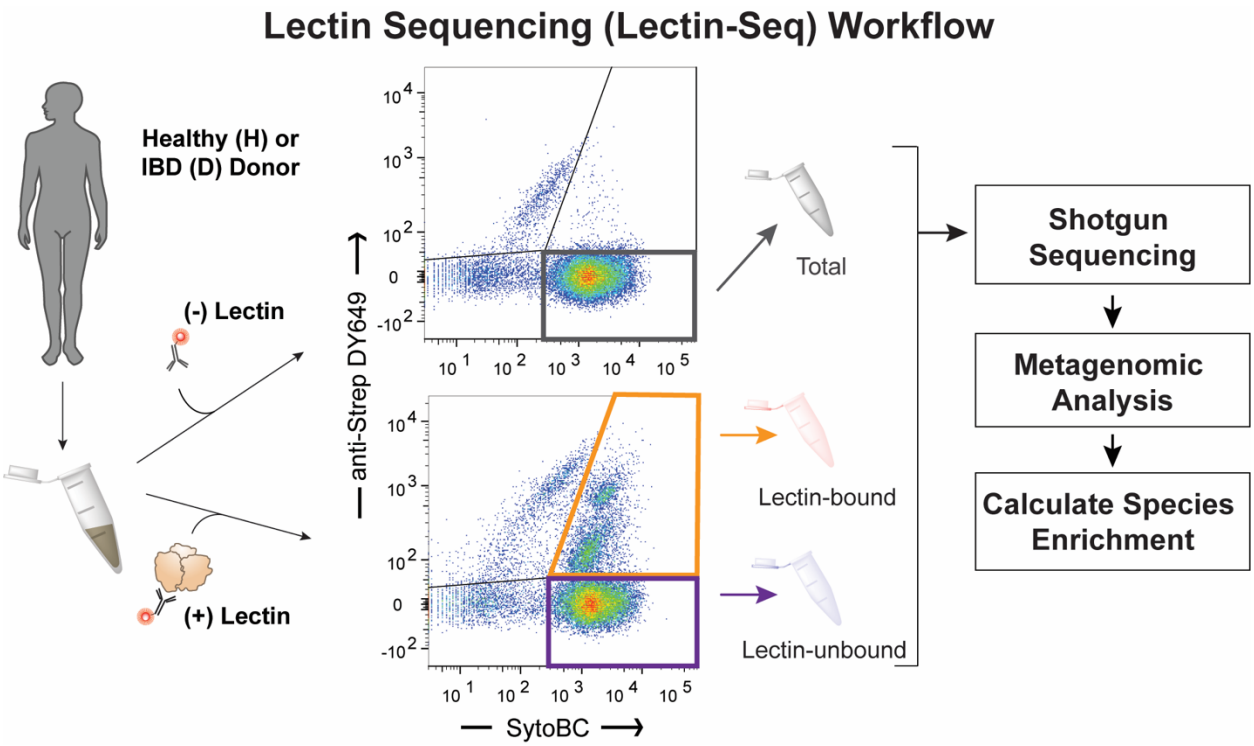

Figure 3. Lectin-Seq schematic. Lectin-Seq workflow for identifying lectin bound microbes from human stool samples.

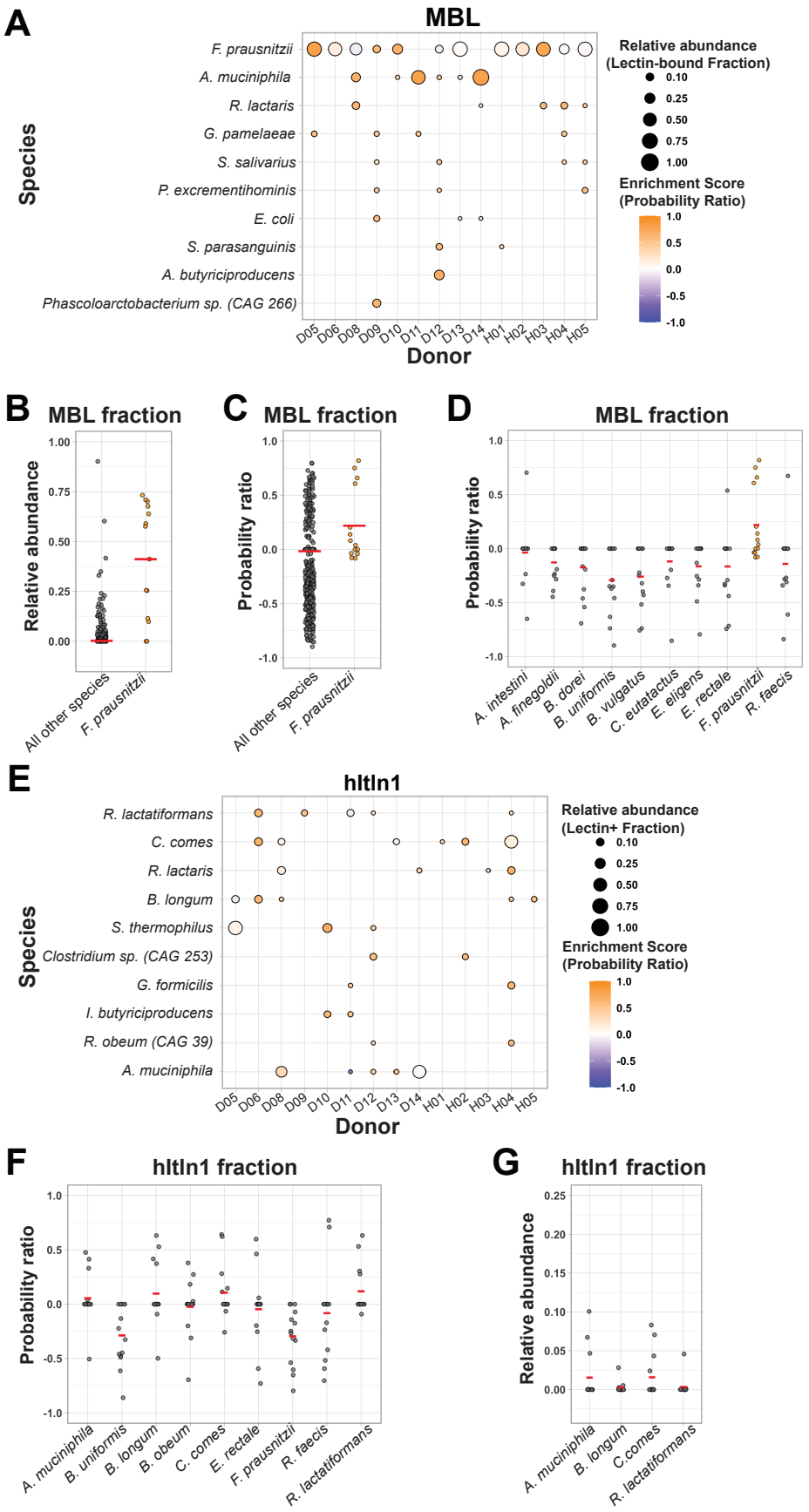
A
MBL
Species
F. prausnitzii
A. muciniphila
R. lactaris
G. pamelaeae
S. salivarius
P. excrementihominis
E. coli
S. parasanguinis
A. butyriciproducens
Phascoloarctobacterium sp. (CAG 266)
D05 D06 D08 D09 D10 D11 D12 D13 D14 H01 H02 H03 H04 H05
Donor
Relative abundance (Lectin-bound Fraction)
0.10
0.25
0.50
0.75
1.00
Enrichment Score (Probability Ratio)
1.0
0.5
0.0
-0.5
-1.0
B
MBL fraction
Relative abundance
All other species
F. prausnitzii
C
MBL fraction
Probability ratio
All other species
F. prausnitzii
D
MBL fraction
Probability ratio
A. intestini
A. finegoldii
B. dorei
B. uniformis
B. vulgatus
C. eutactus
E. eligens
E. rectale
F. prausnitzii
R. faecis
E
hltln1
Species
R. lactatiformans
C. comes
R. lactaris
B. longum
S. thermophilus
Clostridium sp. (CAG 253)
G. formicilis
I. butyriciproducens
R. obeum (CAG 39)
A. muciniphila
D05 D06 D08 D09 D10 D11 D12 D13 D14 H01 H02 H03 H04 H05
Donor
Relative abundance (Lectin+ Fraction)
0.10
0.25
0.50
0.75
1.00
Enrichment Score (Probability Ratio)
1.0
0.5
0.0
-0.5
-1.0
F
hltln1 fraction
Probability ratio
A. muciniphila
B. uniformis
B. longum
B. obeum
C. comes
E. rectale
F. prausnitzii
R. faecis
R. lactatiformans
G
hltln1 fraction
Relative abundance
A. muciniphila
B. longum
C.comes
R. lactatiformans

Figure 4. Identification and quantification of MBL and hItln1 bound bacterial species from human stool samples. (A, E) "Bubble plot" depicting the enrichment of top enriched bacterial species in the lectin-bound fraction (defined as the Probability Ratio) donor stool samples bound by either MBL (A) or hItln1(E). Panels show top enriched bacterial species as calculated by average probability ratio. Probability ratio of each species is represented by the color of each dot, and fractional abundance is represented by the size of the dot. Data shown are from 14 donor stool homogenate samples (9 IBD-diagnosed and 5 healthy donors). (B-C) Dot plot of the (B) relative abundance or (C) probability ratio of *F. prausnitzii* or all other species in the Lectin+ Fraction (MBL+ fraction; n=14). Red line denotes the mean. (D) Dot plot of the probability ratio of top 10 most abundant species (input fraction; n=14) in the MBL+ fraction. Red line denotes the mean. (F) Dot plot of the probability ratio of species bound in >5 hItln1+ fractions across all 14 donor stool homogenates. Red line denotes the mean. (G) Dot plot of the relative abundance (input fraction; n=14) of species with an average $P_R > 0$ (hItln1+ fraction; n=14). Red line denotes the mean.

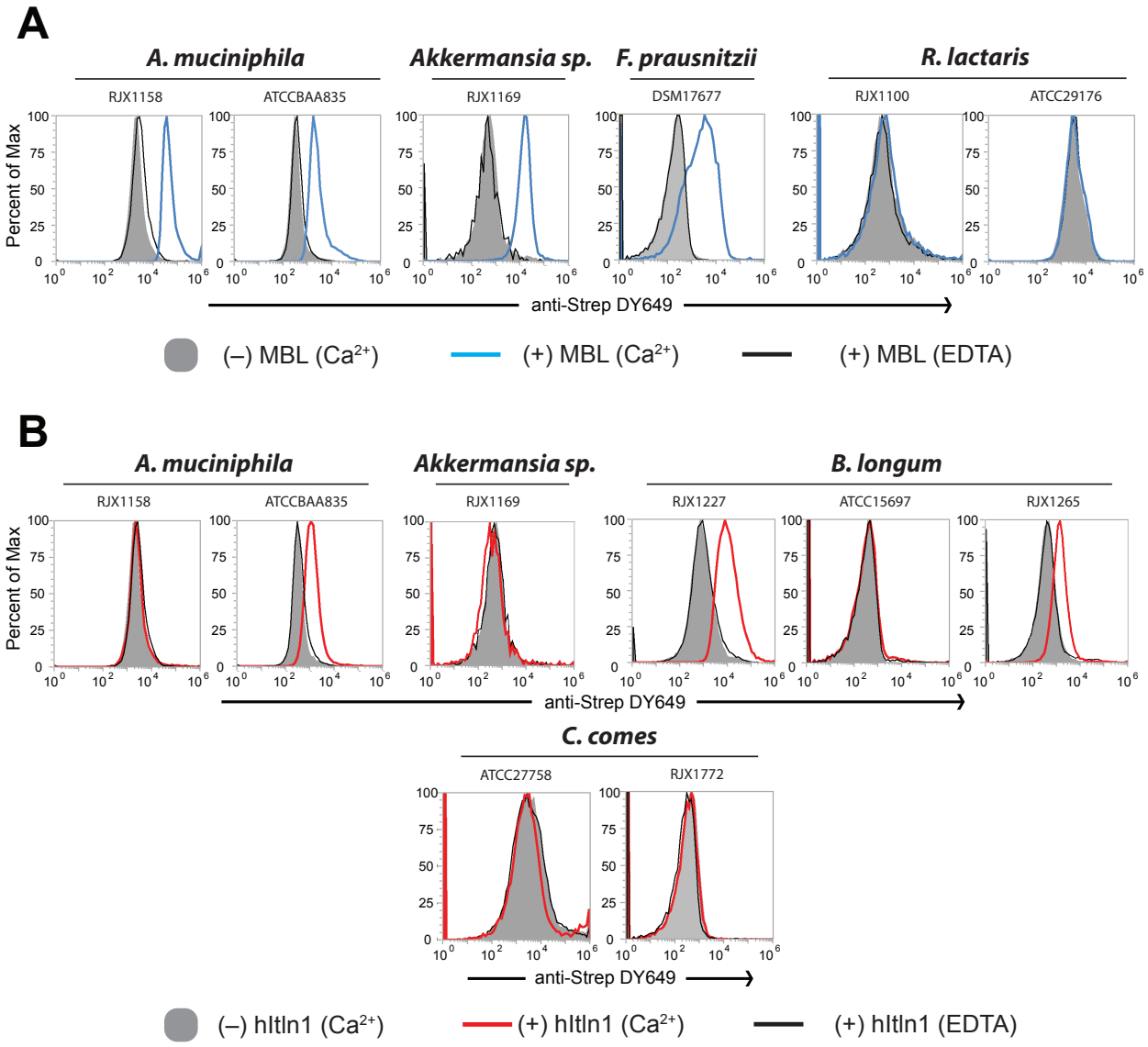

Figure 5. MBL- and hItln1-binding to bacterial isolates. (A-B) Summarized flow cytometry analyses of MBL (A) or hItln1 (B) binding to bacterial isolates. Isolates are grouped by species. Individual histograms plot cell counts as a percent of the maximum signal against lectin binding (anti-Strep DY649). Each plot shows data from (-) lectin (Ca^{2+}; solid grey), (+) MBL/Ca^{2+} (blue trace) or (+) hItln1/Ca^{2+} (red trace), and (+) lectin/EDTA (black trace) binding conditions. Data are representative of two independent experiments.

Supplementary Materials

Supplementary Figures

A

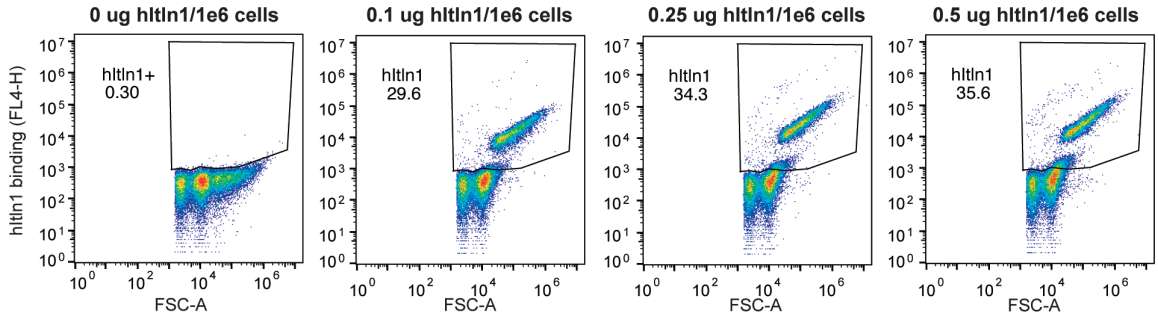

B

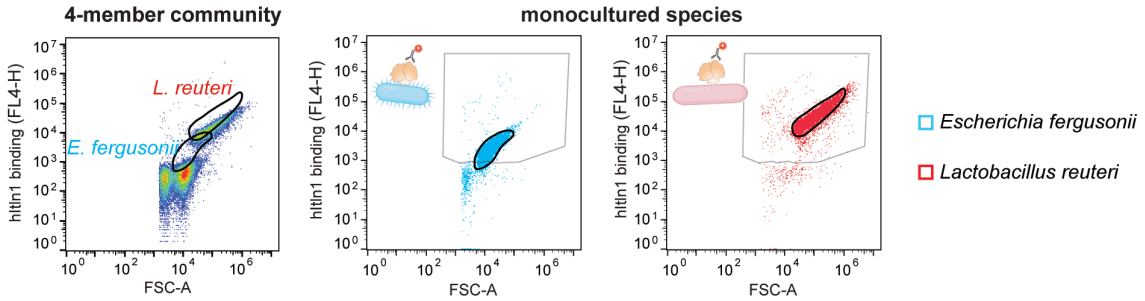

C

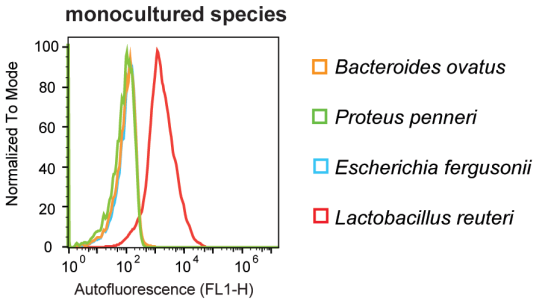

D

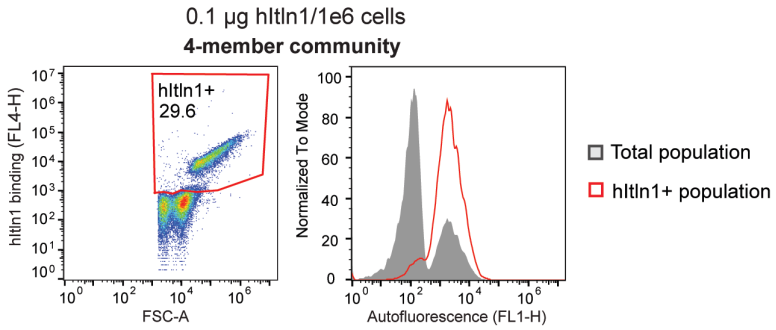

Figure S1. hItln1 binding to synthetic mixed microbial community. (A) Flow cytometry analysis of synthetic mixed microbial community plotted as forward scatter (FSC) against hItln1 binding (FL4-H; anti-Strep Oyster 645). Panels show from (-) lectin/Ca^{2+} and (+) hItln1/Ca^{2+} conditions with increasing concentrations of hItln1. Indicated concentrations refer to the total quantity of hItln1 per 1e6 bacterial cells. Binding assays were done at an approximate cell density between ~5e7 and 1e8 cells/mL. (B) Flow cytometry analysis of synthetic mixed microbial community plotted as forward scatter (FSC) against hItln1 binding (anti-Strep Oyster 645) (data from Figure 1C) indicating the expected scattering patterns of *L. reuteri* and *E. fergusonii*. Panel shown is from 0.1 μg hItln1/1e6 cells condition. hItln1 binding to *L. reuteri* and *E. fergusonii* in monoculture binding assays are shown as reference (data from Figure 1B). (C) Autofluorescence (FL1-H; FITC) of microbial isolates shown as an overlaid histogram. (D) Data shown in Fig. 1C and Fig. S1A with hItln1+ population outlined using a red gate (left panel). Histogram representation of autofluorescence (FL1-H; FITC) of total and hItln1+ populations. Data are representative of two independent experiments.

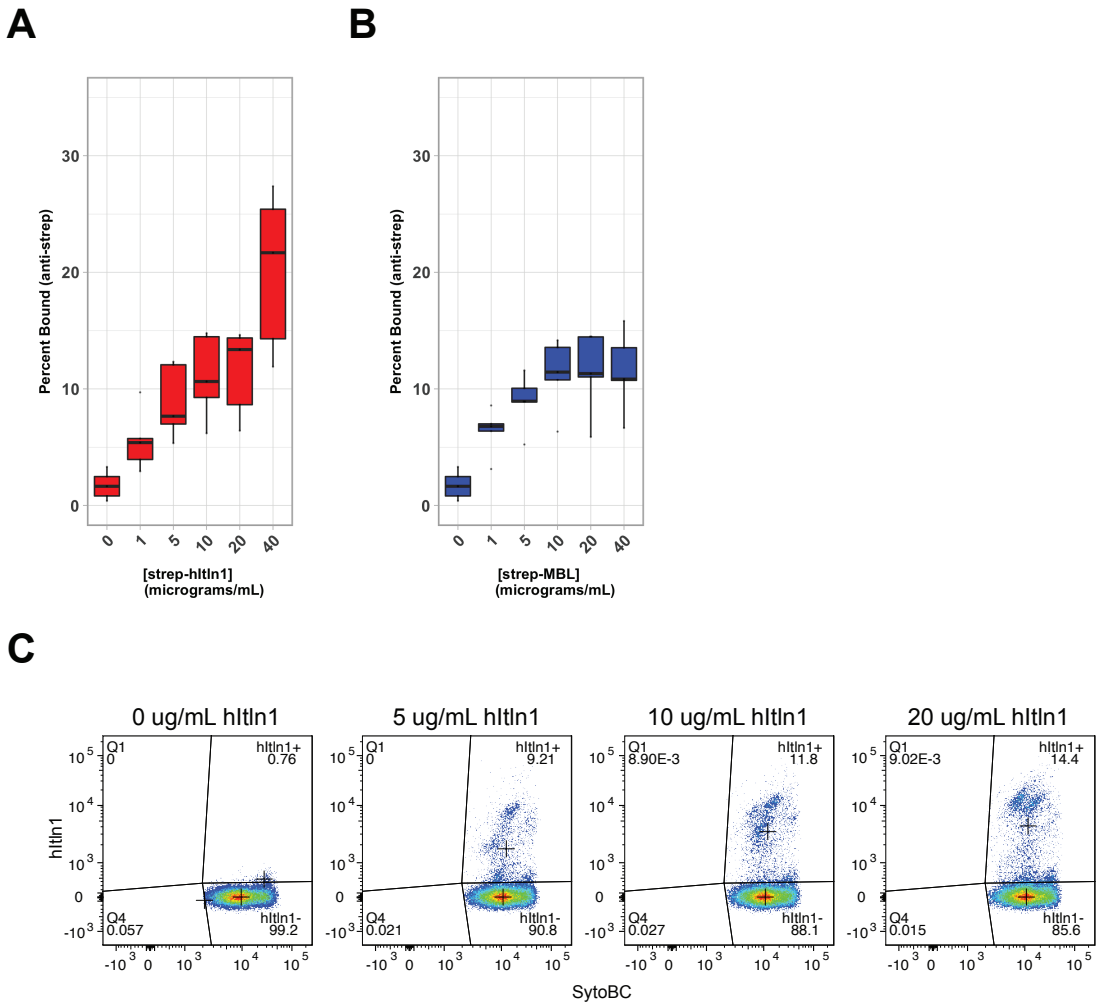

Figure S2. Titration of hItln1 and MBL binding to donor stool samples. (A) Flow cytometry analysis of strep-hItln1 (A) or strep-MBL(B) binding to donor stool samples at different concentrations. Percent bound is calculated by determining the percentage of cells that fall in the strep-pos/SytoBC-pos fraction. Quantification of binding is shown as a boxplot (mean and standard deviation) and reported in Table S3 (mean and standard error of the mean). (C) Flow cytometry analysis of strep-hItln1 binding to donor stool samples at different concentrations plotted as SytoBC against lectin binding (anti-Strep DY649).

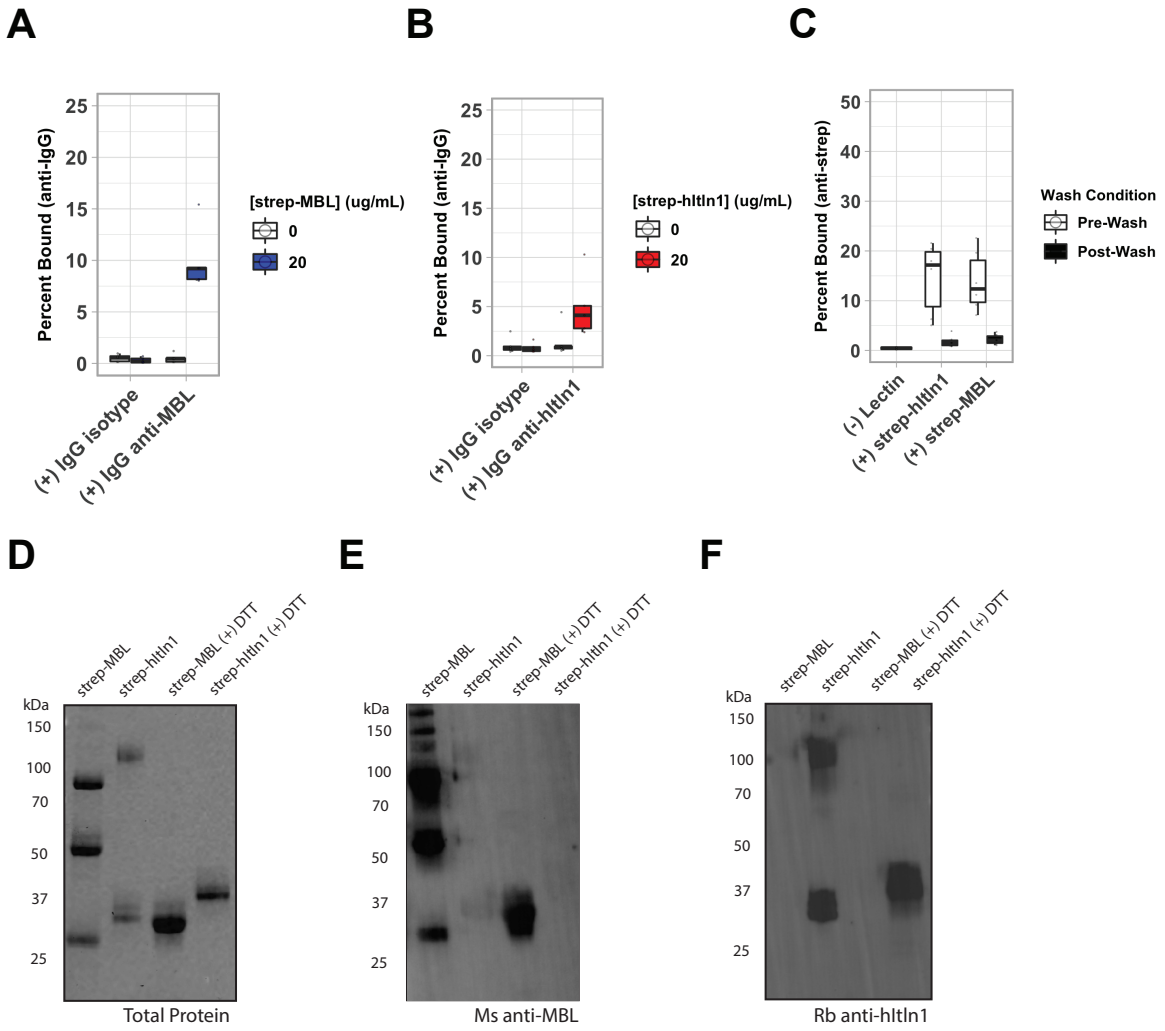

Figure S3. Detection of endogenous MBL and hItln1 on donor stool samples. (A-B) Flow cytometry analysis of IgG anti-MBL (A) or IgG anti-hItln1 (B) staining on donor stool samples. Percent bound is calculated by determining the percentage of cells that fall in the antibody-pos/SytoBC-pos fraction. (A) Quantification (boxplots represent the mean and standard deviation; reported values are mean and standard error of the mean) of staining with IgG isotype controls, IgG anti-MBL alone (n=5; 0.5 +/- 0.1 %) and IgG anti-MBL supplemented with recombinant strep-MBL (n=5; 10.0 +/- 0.6 %). (B) shows staining with IgG isotype controls, IgG anti-hItln1 alone (n=5; 1.5 +/- 0.3 %) and IgG anti-hItln1 supplemented with recombinant strep-hItln1 (n=5; 4.9 +/- 0.6 %). (C) Flow cytometry analysis of levels of donor stool samples stained

with recombinant strep-hItln1 and strep-MBL and analyzed pre- and post-washing with PBS + 12.5% glycerol. Percent bound is calculated by determining the percentage of cells that fall in the antibody-pos/SytoBC-pos fraction. Quantification (boxplots represent the mean and standard deviation; reported values are mean and standard error of the mean) of staining with strep-hItln1 (2nd group) pre- (white; n=5; 14.6 +/- 1.2 %) and post-washing (black; n=5; 1.8 +/- 0.2 %) or strep-MBL (3rd group) pre- (white; n=5; 13.8 +/- 1.0 %) and post-washing (black; n=5; 2.2 +/- 0.2 %). All data are representative of two independent experiments. **(**D) Total protein stain after SDS-PAGE of recombinant strep-MBL or strep-hItln1 in the presence or absence DTT. (E) Western blotting of gel shown in (A) with Ms anti-MBL. (F) Western blotting of gel shown in (A) with Rb anti-hItln1.

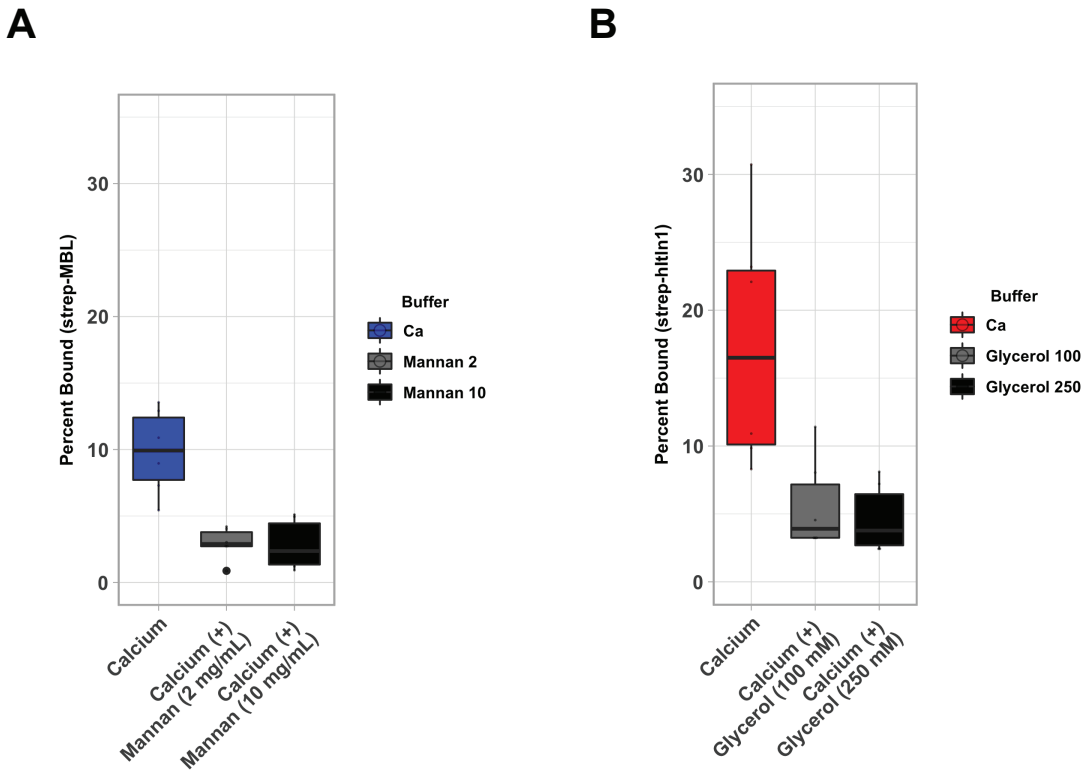

Figure S4. Effect of mannan or glycerol on MBL or hItln1 binding to donor stool samples. (A-B) Flow cytometry analysis of strep-MBL (A) or strep-hItln1(B) binding to donor stool samples in the presence of mannan (MBL) or glycerol (hItln1). Percent bound is calculated by determining the percentage of cells that fall in the strep-pos/SytoBC-pos fraction. (A) Quantification (boxplots represent the mean and standard deviation; reported values are mean and standard error of the mean) of binding with strep-MBL in calcium buffer alone (blue; n=5; 9.8 +/- 0.5 %) or in the presence of mannan at 2 mg/mL (grey; n=5; 2.9 +/- 0.2 %) or 10 mg/mL (black; n=5; 2.8 +/- 0.3%). (B) Quantification (boxplots represent the mean and standard deviation; reported values are mean and standard error of the mean) of binding with strep-hItln1 in calcium buffer alone (red; n=5; 17.5 +/- 1.5 %) or in the presence of glycerol at concentrations of 100 mM (grey; n=5; 5.6 +/- 0.6 %) or 250 mM (black; n=5; 4.6 +/- 0.4%). All data are representative of two independent experiments.

A

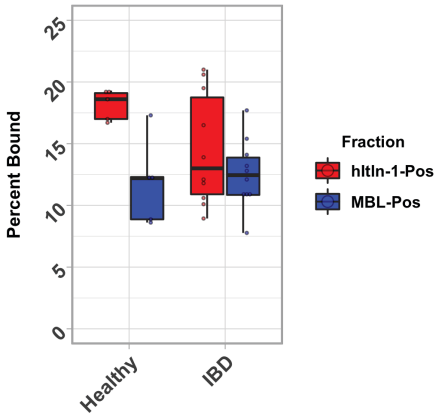

Figure S5. Binding of MBL and hItln1 to healthy or diseased human stool homogenate. (A) Quantification of binding of MBL and hItln1 to human stool homogenate collected from healthy or IBD-diagnosed donors. Percent bound is calculated by determining the percentage of cells that fall in the strep-pos/SytoBC-pos fraction (Q2). Data shown (boxplots represent the mean and standard deviation; reported values are mean and standard error of the mean) are from healthy donor samples bound by (+) strep-hItln1/Ca^{2+} (red; n=5; 18.1 +/- 0.5 %) and (+) strep-MBL/Ca^{2+} (blue; n=5; 11.9 +/- 1.6 %) or IBD-diagnosed donor samples bound by (+) strep-hItln1/Ca^{2+} (red; n=9; 14.5 +/- 1.4 %) and (+) strep-MBL/Ca^{2+} (blue; n=9; 12.6 +/- 0.9 %).

A

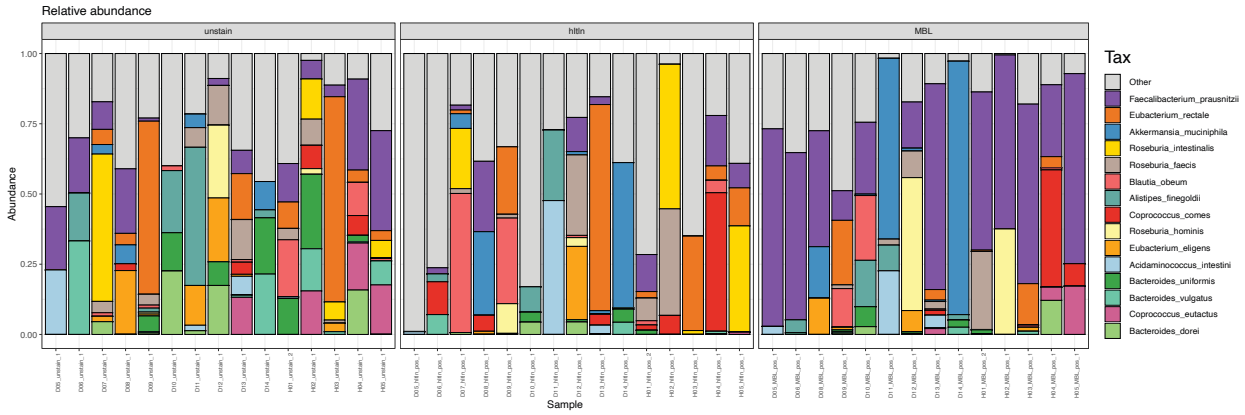

Figure S6. Fraction of bacterial species in input or lectin-bound fractions of human stool samples. Fractional abundance of bacterial species in the input (panel 1), MBL-bound (panel 2) or hItln1-bound (panel 3) fractions from 14 donor stool homogenate samples (9 IBD-diagnosed and 5 healthy donors). Each column represents a different sample and species are represented by indicated colors.

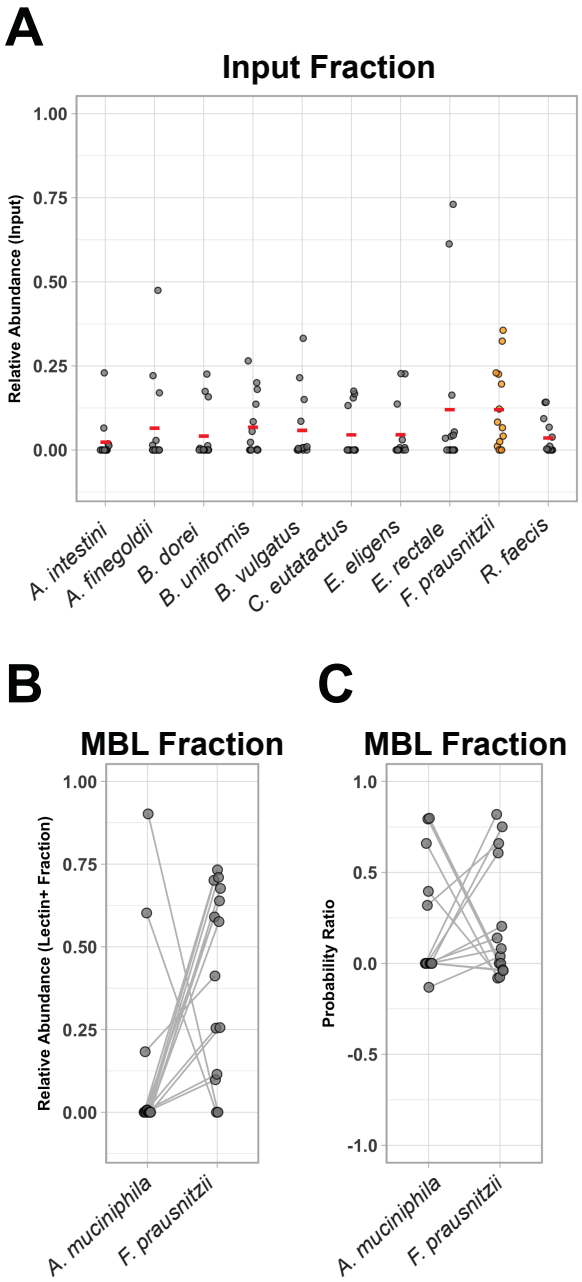

Figure S7. Abundance of bacterial species in input or MBL-bound fractions of human stool samples. (A) Dot plot of the relative abundance of top 10 most abundant species in the input fraction across all donor stool homogenate samples (n=14; 9 IBD-diagnosed and 5 healthy donors). (B-C) Relative abundances (B) or probability ratios (C) of *A. muciniphila* and *F. prausnitzii* in the lectin-bound fraction (MBL+ fraction; n=14). Lines connect data points that come from the same sample.

A
MBL
Tyzzerella_nexilis
Turicimonas_muris
Streptococcus_thermophilus
Streptococcus_salivarius
Streptococcus_parasanguinis
Slackia_isoflavoniconvertens
Ruthenibacterium_lactatiformans
Ruminococcus_torques
Ruminococcus_obeum_CAG_39
Ruminococcus_lactaris
Ruminococcus_gnavus
Ruminococcus_champanellensis
Ruminococcus_bromii
Ruminococcus_bicirculans
Roseburia_intestinalis
Roseburia_hominis
Roseburia_faecis
Phascolarctobacterium_succinatutens
Phascolarctobacterium_sp_CAG_266
Phascolarctobacterium_faecium
Parasutterella_excrementihominis
Parabacteroides_merdae
Parabacteroides_distasonis
Oscillibacter_sp_CAG_241
Oscillibacter_sp_57_20
Monoglobus_pectinilyticus
Holdemanella_biformis
Gordonibacter_pamelaeae
Gemmiger_formicilis
Fusicatenibacter_saccharivorans
Firmicutes_bacterium_CAG_110
Faecalibacterium_prausnitzii
Eubacterium_sp_CAG_38
Eubacterium_sp_CAG_180
Eubacterium_siraeum
Eubacterium_rectale
Eubacterium_limosum
Eubacterium_hallii
Eubacterium_eligens
Eubacterium_callanderi
Escherichia_coli
Erysipelothrix_larvae
Eisenbergiella_massiliensis
Eggerthella_lenta
Dorea_sp_CAG_317
Dorea_longicatena
Dialister_sp_CAG_357
Dialister_invisus
Coprococcus_eutactus
Coprococcus_comes
Collinsella_stercoris
Collinsella_intestinalis
Collinsella_aerofaciens
Clostridium_sp_CAG_58
Clostridium_clostridioforme
Clostridium_bolteae_CAG_59
Clostridium_bolteae
Clostridium_asparagiforme
Cloacibacillus_porcorum
Blautia_wexlerae
Blautia_sp_CAG_257
Blautia_obeum
Blastocystis_sp_subtype_1
Bifidobacterium_pseudocatenulatum
Bifidobacterium_longum
Bifidobacterium_bifidum
Bifidobacterium_adolescentis
Barnesiella_intestinihominis
Bacteroides_vulgatus
Bacteroides_uniformis
Bacteroides_thetaiotaomicron
Bacteroides_stercoris
Bacteroides_salyersiae
Bacteroides_plebeius
Bacteroides_ovatus
Bacteroides_intestinalis
Bacteroides_faecis
Bacteroides_eggerthii
Bacteroides_dorei
Bacteroides_caccae
Anaerotignum_lactatifermentans
Alistipes_shahii
Alistipes_putredinis
Alistipes_finegoldii
Akkermansia_muciniphila
Agathobaculum_butyriciproducens
Acidaminococcus_intestini
Species
D05 D06 D08 D09 D10 D11 D12 D13 D14 H01 H02 H03 H04 H05
Sample
Relative Abundance (Enriched Fraction)
0.10
0.25
0.50
0.75
1.00
PR Ratio
1.0
0.5
0.0
-0.5
-1.0
B
hltln1
Tyzzerella_nexilis
Turicimonas_muris
Streptococcus_thermophilus
Streptococcus_salivarius
Streptococcus_parasanguinis
Streptococcus_mitis
Slackia_isoflavoniconvertens
Ruthenibacterium_lactatiformans
Ruminococcus_obeum_CAG_39
Ruminococcus_lactaris
Ruminococcus_gnavus
Ruminococcus_champanellensis
Ruminococcus_bromii
Ruminococcus_bicirculans
Roseburia_intestinalis
Roseburia_hominis
Roseburia_faecis
Pseudomonas_yamanorum
Proteobacteria_bacterium_CAG_139
Phascolarctobacterium_sp_CAG_266
Parasutterella_excrementihominis
Parabacteroides_merdae
Parabacteroides_distasonis
Oscillibacter_sp_CAG_241
Oscillibacter_sp_57_20
Odoribacter_splanchnicus
Monoglobus_pectinilyticus
Lactobacillus_sakei
Lachnospira_pectinoschiza
Intestinimonas_butyriciproducens
Gemmiger_formicilis
Fusicatenibacter_saccharivorans
Flavonifractor_plautii
Firmicutes_bacterium_CAG_110
Faecalibacterium_prausnitzii
Eubacterium_sp_CAG_38
Eubacterium_sp_CAG_180
Eubacterium_siraeum
Eubacterium_rectale
Eubacterium_ramulus
Eubacterium_eligens
Eisenbergiella_massiliensis
Dialister_sp_CAG_357
Coprococcus_eutactus
Coprococcus_comes
Collinsella_stercoris
Collinsella_intestinalis
Collinsella_aerofaciens
Clostridium_sp_CAG_58
Clostridium_sp_CAG_411
Clostridium_sp_CAG_253
Clostridium_leptum
Clostridium_lavalense
Clostridium_clostridioforme
Clostridium_bolteae_CAG_59
Clostridium_bolteae
Clostridium_asparagiforme
Clostridiales_bacterium_1_7_47FAA
Cloacibacillus_porcorum
Blautia_wexlerae
Blautia_sp_CAG_257
Blautia_obeum
Blastocystis_sp_subtype_1
Bilophila_wadsworthia
Bifidobacterium_pseudocatenulatum
Bifidobacterium_longum
Bifidobacterium_bifidum
Bifidobacterium_adolescentis
Barnesiella_intestinihominis
Bacteroides_xylanisolvens
Bacteroides_vulgatus
Bacteroides_uniformis
Bacteroides_salyersiae
Bacteroides_plebeius
Bacteroides_ovatus
Bacteroides_massiliensis
Bacteroides_intestinalis
Bacteroides_fragilis
Bacteroides_faecis
Bacteroides_eggerthii
Bacteroides_dorei
Bacteroides_caccae
Anaerostipes_hadrus
Alistipes_shahii
Alistipes_putredinis
Alistipes_inops
Alistipes_finegoldii
Akkermansia_muciniphila
Acidaminococcus_intestini
Species
D05 D06 D08 D09 D10 D11 D12 D13 D14 H01 H02 H03 H04 H05
Sample
Relative Abundance (Enriched Fraction)
0.10
0.25
0.50
0.75
1.00
PR Ratio
1.0
0.5
0.0
-0.5
-1.0

Figure S8. Probability ratios of MBL and hItln1 enrichments of bacterial species from human stool samples. "Bubble plot" depicting the enrichment of all enriched bacterial species in the lectin-bound fraction (defined as the Probability Ratio) donor stool samples bound by either MBL (A) or hItln1 (B). Probability ratio of each species is represented by the color of each dot, and fractional abundance is represented by the size of the dot. Data shown are from 14 donor stool homogenate samples (9 IBD-diagnosed and 5 healthy donors).

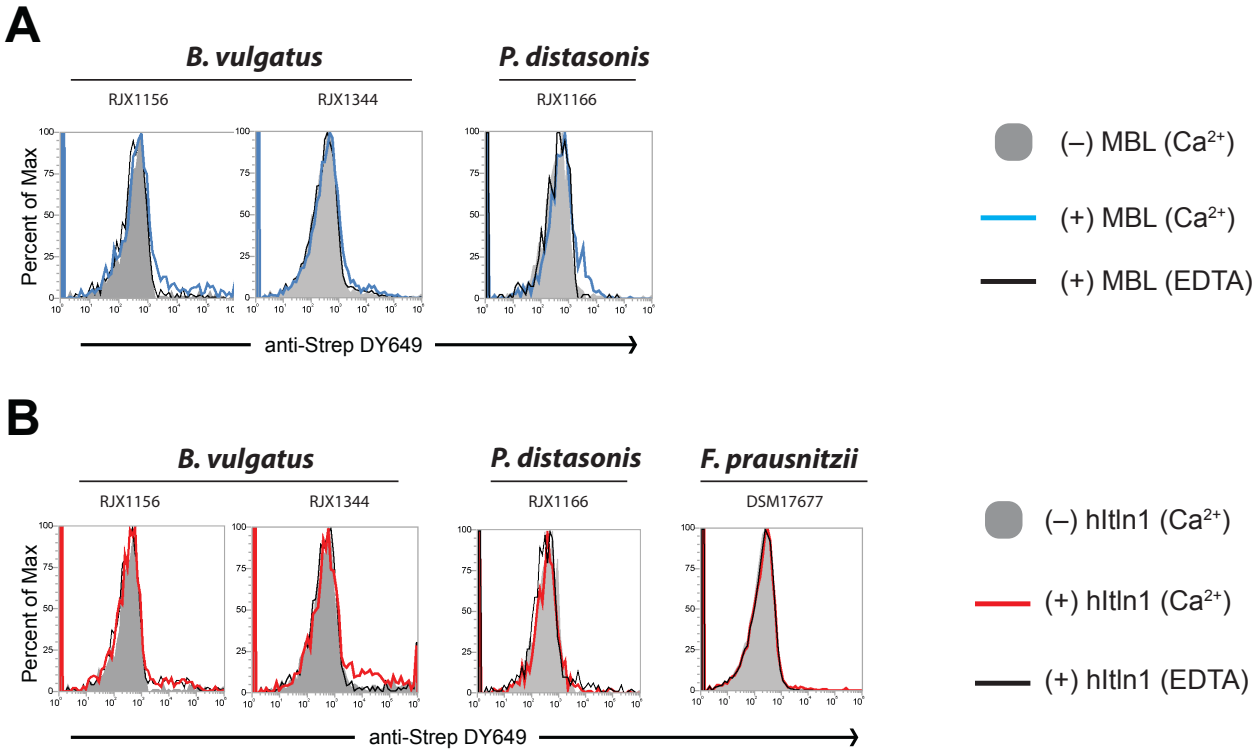

Figure S9. MBL or hItln1 binding to negative control bacterial isolates. (A-B) Summarized flow cytometry analyses of MBL (A) or hItln1 (B) binding to bacterial isolates. Isolates are grouped by species. Individual histograms plot cell counts as a percent of the maximum signal against lectin binding (anti-Strep DY649). Each plot shows data from (-) lectin (Ca^{2+}; solid grey), (+) MBL/Ca^{2+} (blue trace) or hItln1/Ca^{2+} (red trace), and (+) lectin/EDTA (black trace) binding conditions. Data are representative of two independent experiments.

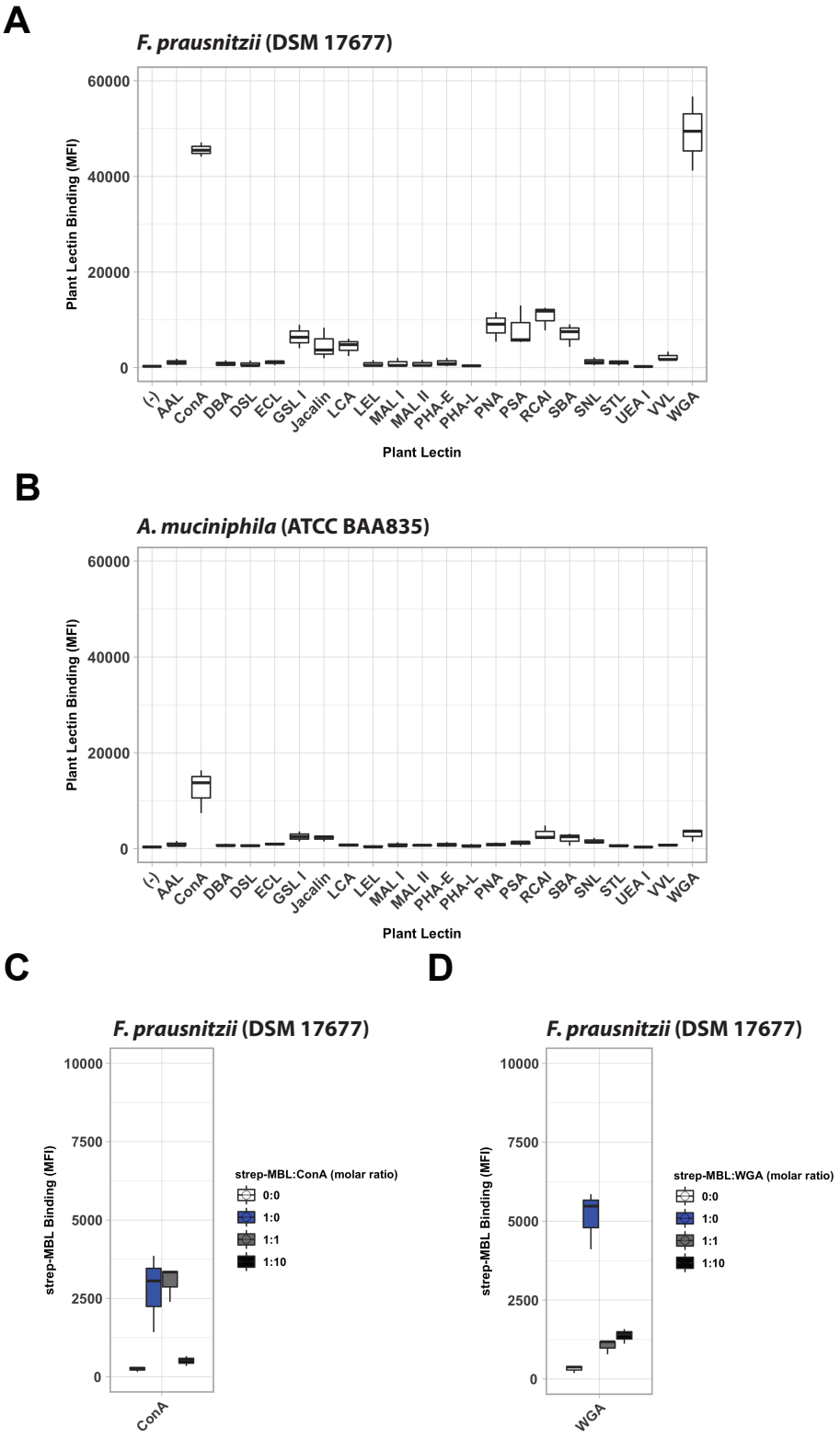

Figure S10. Plant lectin binding to microbial isolates. (A-B) Flow cytometry analysis of binding by biotinylated plant lectins (measured by Strep-Tactin XT DY-649) to *F. prausnitzii*

isolate DSM 17677 (A) and *A. muciniphila* ATCC BAA835 (B). Quantification (boxplots represent the mean and standard deviation) of binding is shown as MFI and is reported in Table S7. (C-D) Flow cytometry analysis of strep-MBL binding to DSM 17677 in the presence of unlabeled ConA and WGA. (C) Quantification (boxplots represent the mean and standard deviation; reported values are mean and standard error of the mean) of DSM 17677 staining (MFI) by strep-MBL alone (blue; n=3; 2783 +/- 413) or in the presence of ConA at a 1:1 (grey; n=3; 3037 +/- 186) or 10:1 (black; n = 511 +/- 53) ratio. (D) Quantification (boxplots represent the mean and standard deviation; reported values are mean and standard error of the mean) of DSM 17677 staining (MFI) by strep-MBL alone (blue; n=3; 5148 +/- 306) or in the presence of WGA at a 1:1 (grey; n=3; 1047 +/- 76) or 10:1 (black; n = 1370 +/- 78) ratio. All data are representative of two independent experiments.

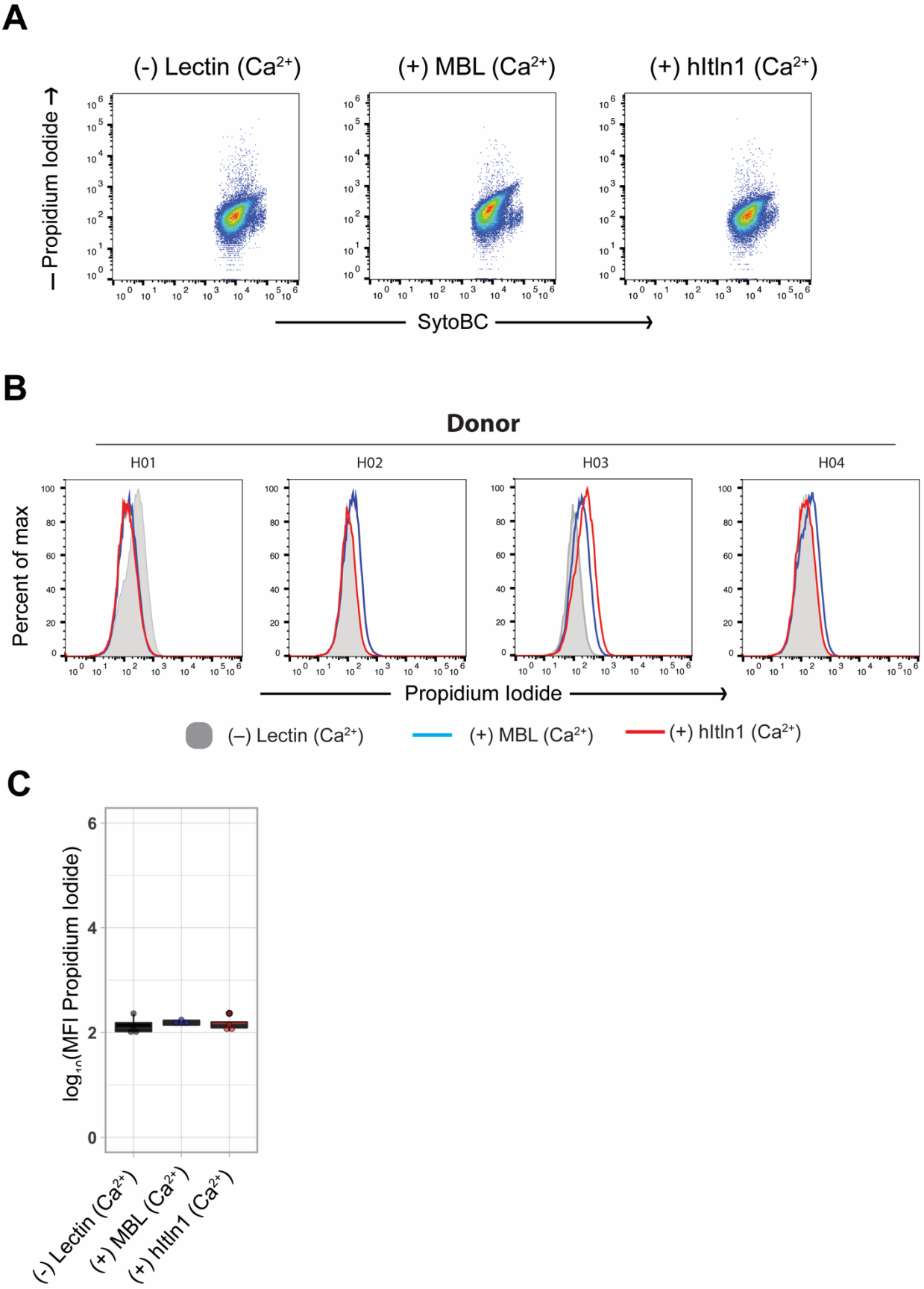
A
(-) Lectin (Ca2+)
(+) MBL (Ca2+)
(+) hItln1 (Ca2+)
Propidium Iodide
SytoBC
B
Donor
H01
H02
H03
H04
Percent of max
Propidium Iodide
(–) Lectin (Ca2+)
(+) MBL (Ca2+)
(+) hItln1 (Ca2+)
C
log10(MFI Propidium Iodide)
(-) Lectin (Ca2+)
(+) MBL (Ca2+)
(+) hItln1 (Ca2+)

Figure S11. Effect of MBL and hItln1 binding on microbial cell viability. (A) Representative flow cytometry analysis of healthy human stool homogenate (Donor H01) plotted as SytoBC against propidium iodide. Panels show no lectin control, (+) MBL (Ca^{2+}) and (+) hItln1 (Ca^{2+}) conditions. (B) Representative flow cytometry analyses showing the effect of lectin binding on propidium iodide staining of healthy human stool homogenate sample (Donor H01). Individual histograms plot cell counts as a percent of the maximum signal against propidium iodide. Each plot shows data from (-) lectin (Ca^{2+}; solid grey), (+) MBL/Ca^{2+} (blue trace) or hItln1/Ca^{2+} (red trace). Data from (A) and (B) are representative of data collected with remaining donor stool homogenate samples (C) Quantification of data shown in A. Data shown (boxplots represent the mean and standard deviation; reported values are mean and standard error of the mean) are the mean fluorescence intensities of propidium iodide in the (-) lectin control (black; n=4; 135.3 +/- 30.1 (mean, SEM)), (+) MBL (Ca^{2+}) (blue; n=4; 154.9 +/- 9.5) and (+) hItln1 (Ca^{2+}) (red; n=4; 145.6 +/- 27.8) samples.

Supplemental Tables

Table S1. Species, strain name and hItln1 binding summary of microbial isolates shown in Fig. 1.

Table S2. Raw glycan array data shown in Fig. 2D.

Table S3. Quantification of titration of data shown in Fig. S2

Table S4. Abundance and enrichment of microbial species in Lectin-Seq fractions.

Table S5. Stool sample metadata.

Table S6. Metadata of microbial isolates shown in Fig. 5 and Fig. S9

Table S7. Details of plant lectin binding to microbial isolates shown in Fig. S10

Table S8. Graphic representation of glycans on microbial glycan array. Sourced from NCFG (*47*)